Supplementary Information

Controlling aromatic helix dimerization in water by tuning charge repulsions

Binhao Teng, [a] Pradeep K. Mandal, [a] Lars Allmendinger, [a] Céline Douat,[a] Yann Ferrand [b] and Ivan Huc* [a]

[a.] Department of Pharmacy, Ludwig-Maximilians-Universität, Butenandtstr. 5–13, 81377, München, Germany.

[b.] Univ. Bordeaux, CNRS, Bordeaux Institut National Polytechnique, CBMN UMR 5248, 2 rue Escarpit, 33600 Pessac, France.

Table of contents

1 Supplementary Schemes and Figures

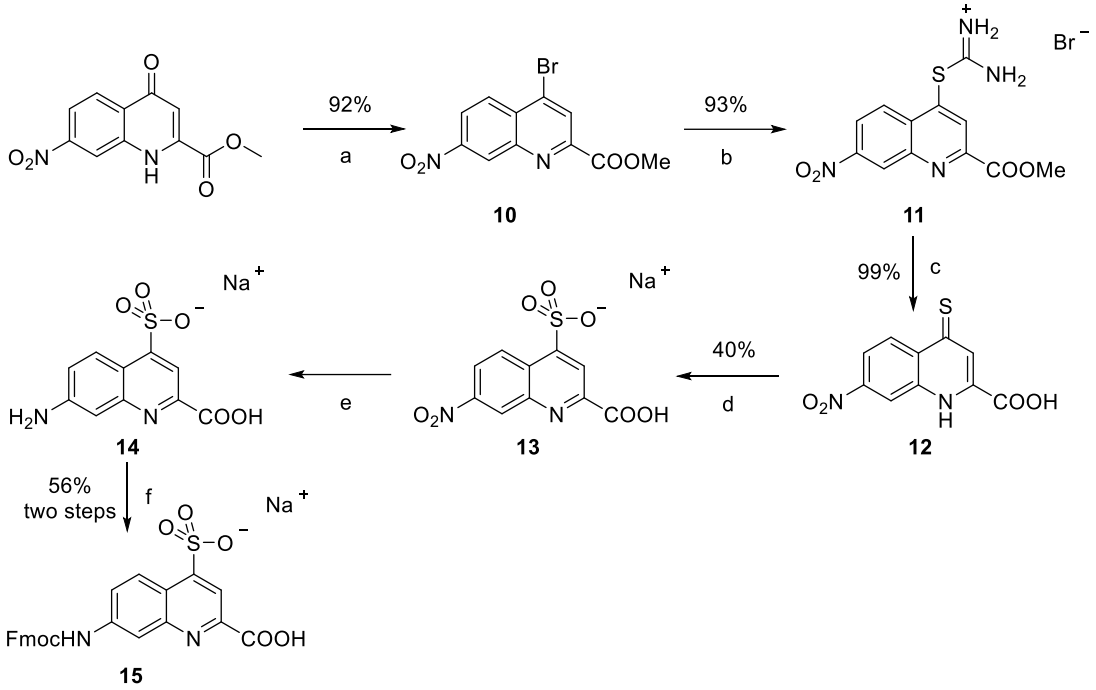

Scheme S1. Synthesis of **Qh^{Sul}** monomer: a) $POBr_3$, DMF; b) thiourea, acetone, reflux; c) NaOH, MeOH/H_2O, r.t.; d) 30% H_2O_2, formic acid, 0 °C; e) Pd/C, H_2, MeOH; f) Fmoc-Cl, $NaHCO_3$, dioxane, H_2O, 0 °C to r.t..

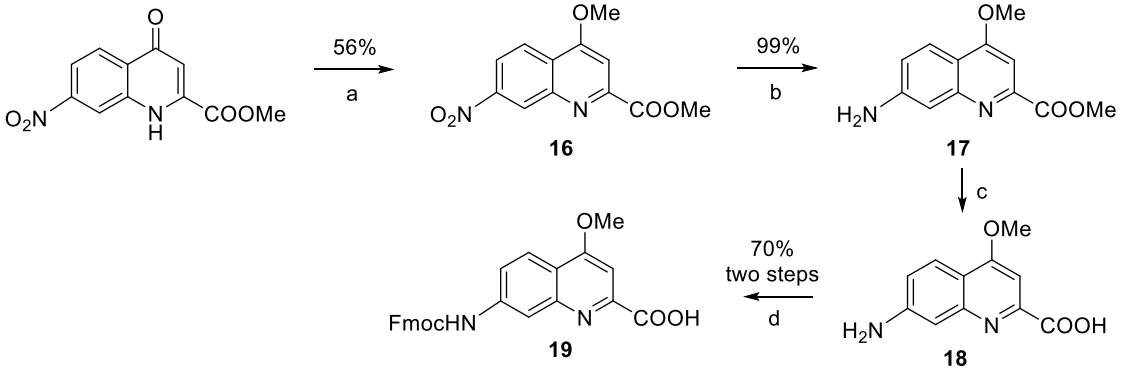

Scheme S2. Synthesis of **Qh^{Ala}** monomer: a) Pd/C, H_2, MeOH/THF; b) LiOH, THF, H_2O, 0 °C; c) Fmoc-Cl, $NaHCO_3$, dioxane, H_2O, 0 °C to r.t..

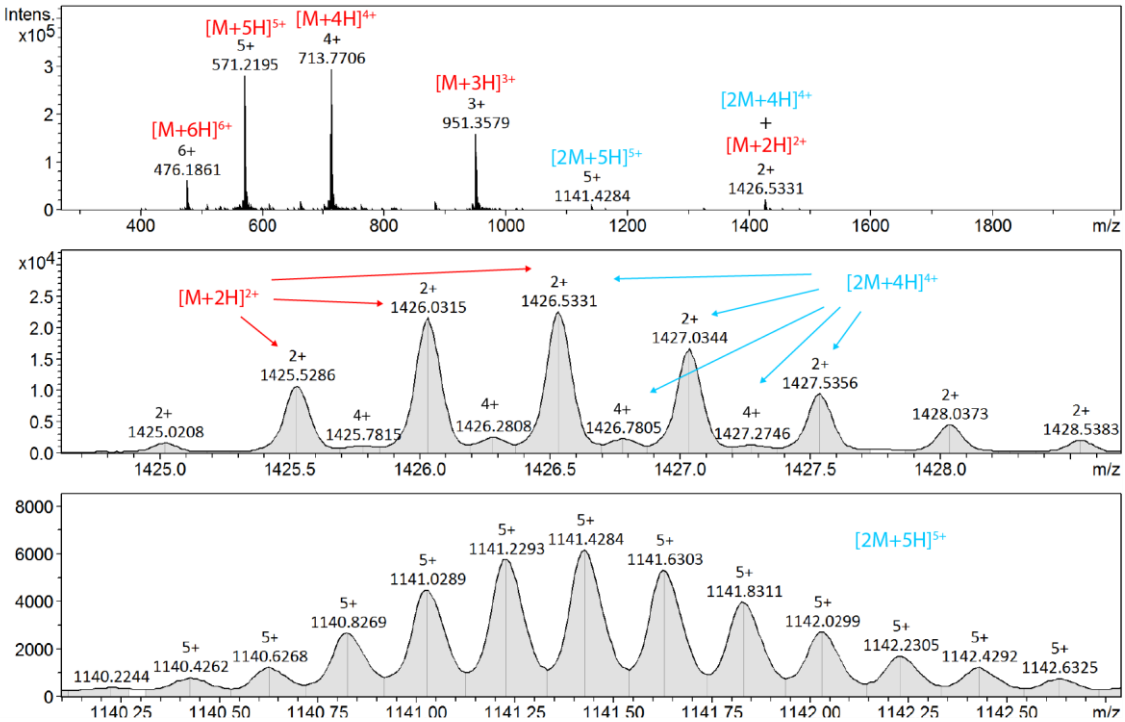

Figure S1. ESI-MS spectrum of oligomer 2 (direct infusion of an aqueous sample). Peaks corresponding to monomeric and dimeric species are highlighted in red and blue, respectively. The $[M+2H]^{2+}$ peak is superimposed by the $[2M+4H]^{4+}$ peak.

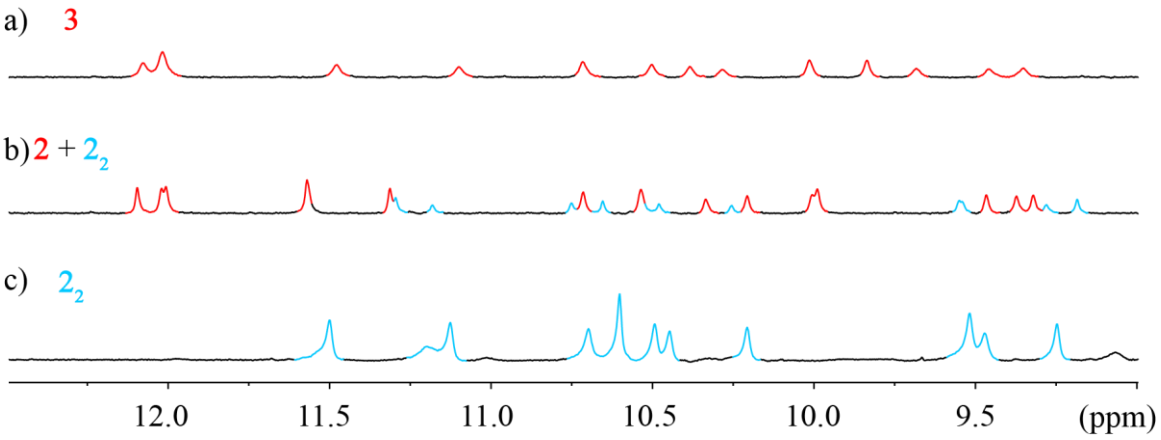

Figure S2. The comparison between oligomer 3 and monomeric oligomer 2. Excerpts of ^{1}H NMR (500 MHz, water suppression) at 25 °C: a) **3** at 0.5 mM and **2** at b) 0.5 mM and c) 4 mM in 45 mM sodium acetate aqueous buffer pH 4.0. Signals corresponding to monomeric and dimeric species are highlighted in red and blue, respectively.

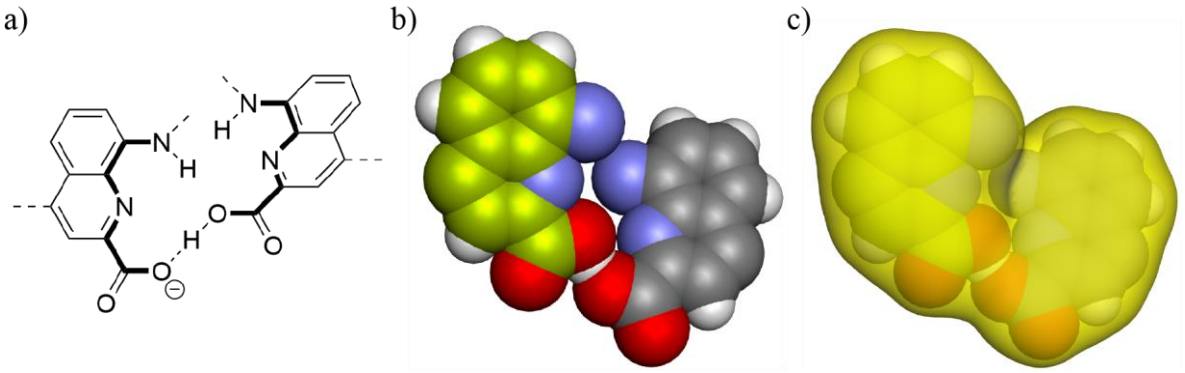

Figure S3. Computational analysis of the fragment of the helix–helix binding interface. The models showed the C-terminal monomers in space-filling representation in a) chemical structural formula, b) energy minimized model in CPK style and c) the calculated solvent accessible surface. Side chains are omitted for clarity. Solvent-accessible surface area was calculated using discovery studio software with a radius of 1.4 Å. The assignment of the carboxylic acid and carboxylate function is tentative, based on orientation.

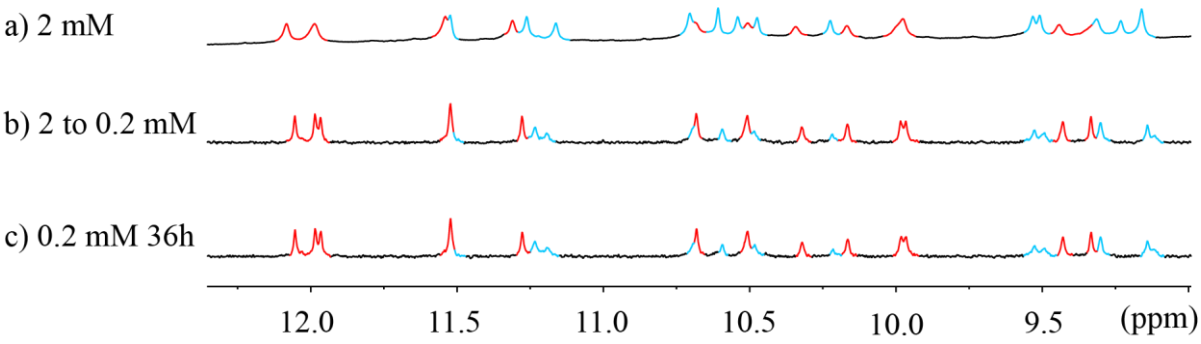

Figure S4. Dilution experiments of oligomer 2. Excerpts of ^{1}H NMR (500 MHz, water suppression) at 25 °C of oligomer **2** in H_2O/D_2O (9:1, *v*/*v*). a) no difference in NMR of **2** at 2 mM was observed in variable incubation time (0.5 h, 1 h and 4 h, only 4 h is shown). b) The NMR was immediately measured after diluting 2 mM of **2** to 0.2 mM and showed dimer to monomer equilibrium. c) A diluted solution of **2** was incubated for 36 h and showed no proportion change between the two species. This means that **2** reached monomer-dimer equilibrium immediately upon being dissolved . Peaks corresponding to monomeric and dimeric species are highlighted in red and blue, respectively.

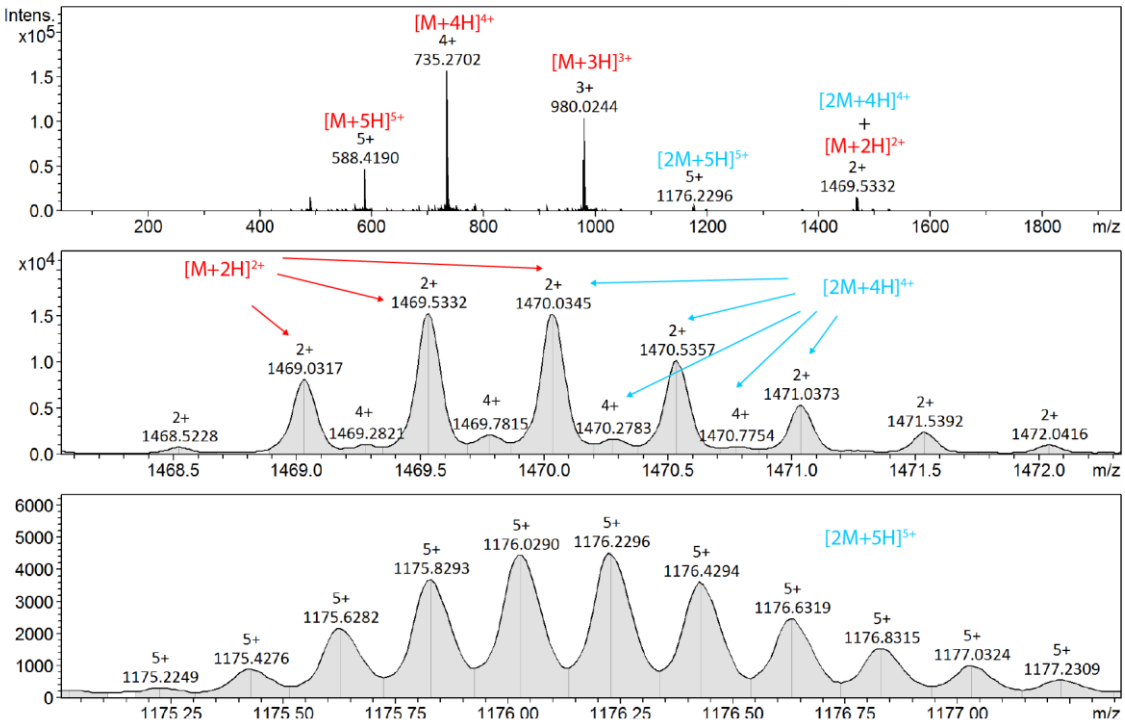

Figure S5. ESI-MS spectrum of oligomer 4 (direct infusion of an aqueous sample). Peaks corresponding to monomeric and dimeric species are highlighted in red and blue, respectively. The $[M+2H]^{2+}$ peak is superimposed by the $[2M+4H]^{4+}$ peak.

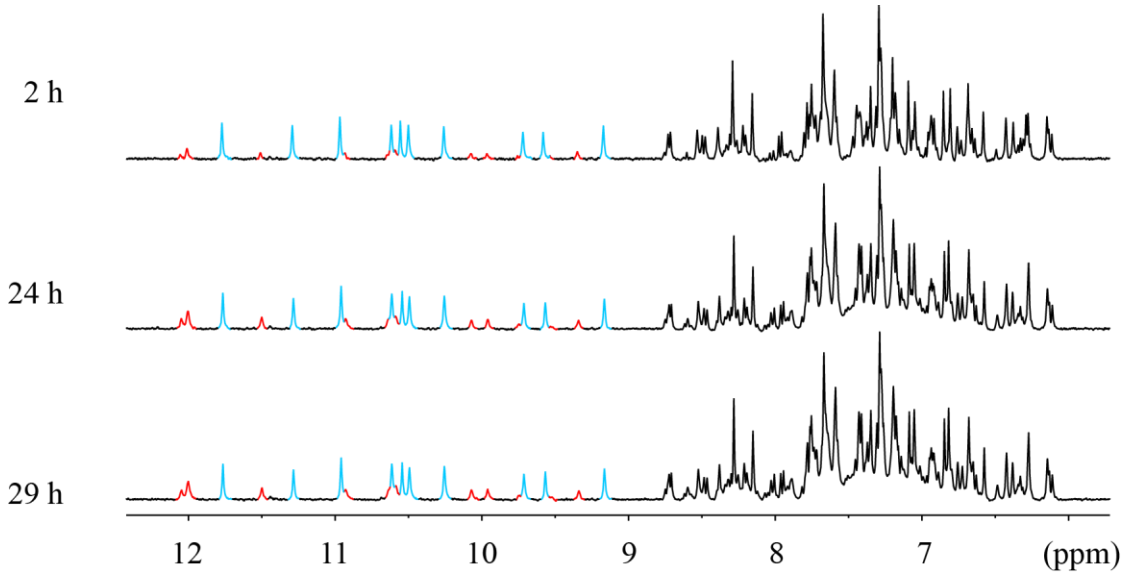

Figure S6. Variable incubation time ^{1}H NMR spectra of 4. Excerpts of ^{1}H NMR (500 MHz, water suppression) at 25 °C of oligomer **4** at 0.5 mM in 13.5 mM sodium acetate aqueous buffer pH 4.0 obtained after varying incubation times. Signals corresponding to monomeric and dimeric species are highlighted in red and blue, respectively.

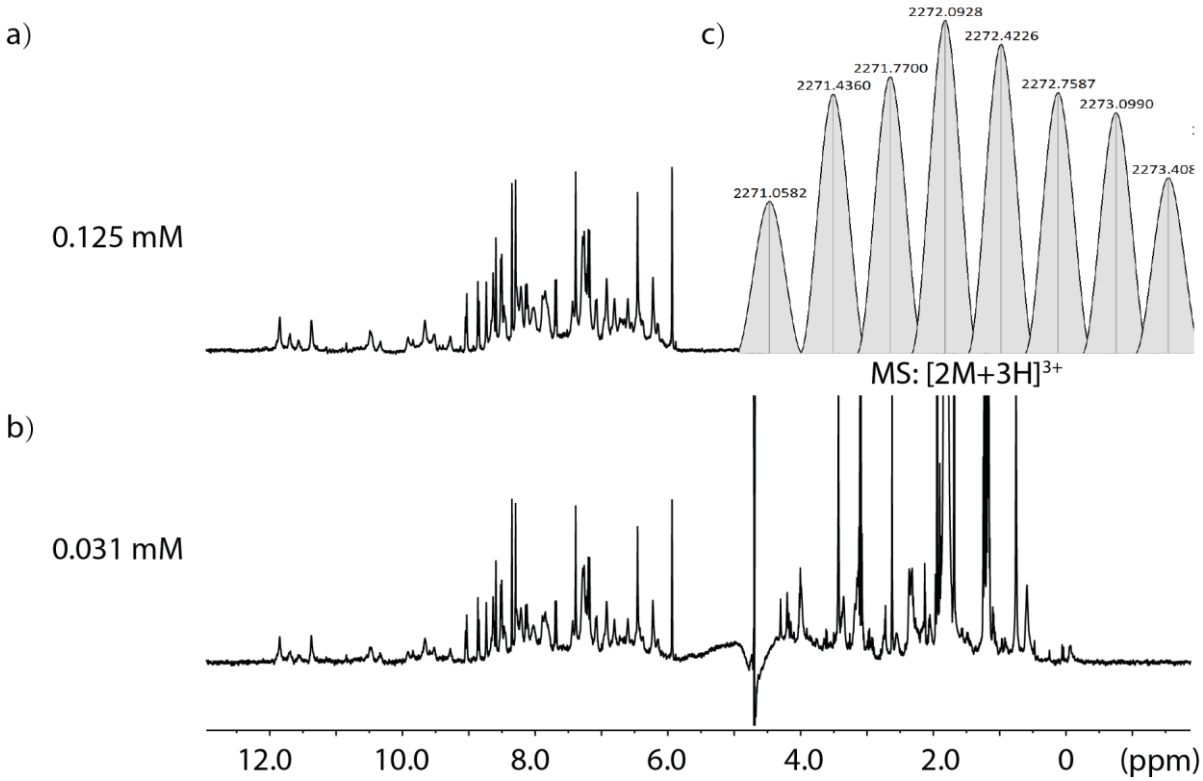

Figure S7. ^{1}H NMR spectra of oligomer 5 in buffered water. ^{1}H NMR spectrum of oligomer **5** at 0.125 mM (a) and 0.031 mM (b) with water suppression (500 MHz, 13 mM ammonium acetate aqueous buffer pH 8.5/D_2O (9:1, *v*/*v*), 25 °C). An extract of the mass spectrum of **5** highlighting the presence of a dimeric species is shown in c).

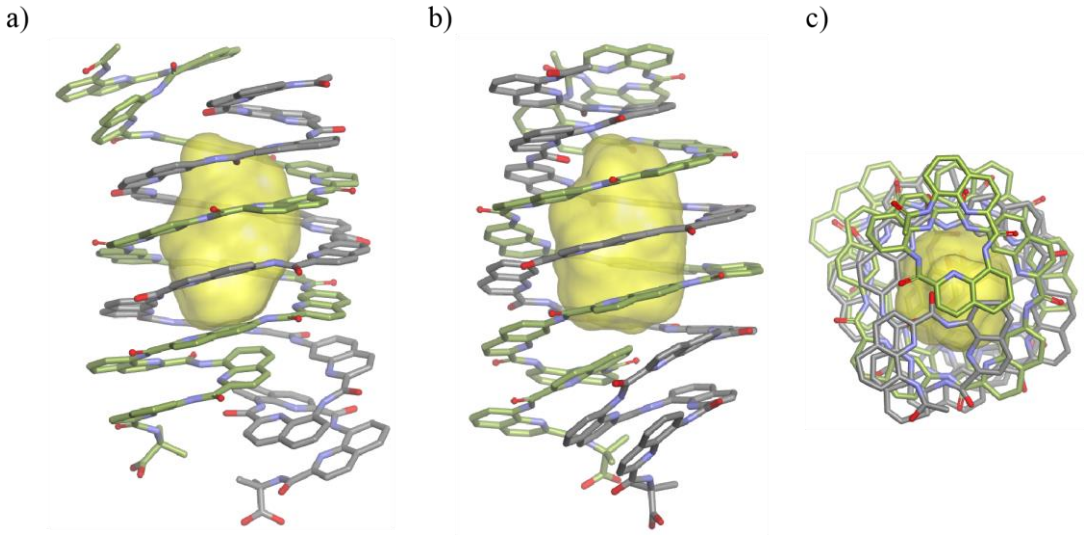

Figure S8. Cavity volume calculation of (5)$_2$. The front view, side view, and top view of (**5**)$_2$ are shown in tube representation where the cavity volume of 346 Å^3 is shown as a transparent yellow isosurface (a, b, c). In all representations, each strand is colored in green and grey, respectively. Side chains and N-terminal Deg tail were omitted for clarity.

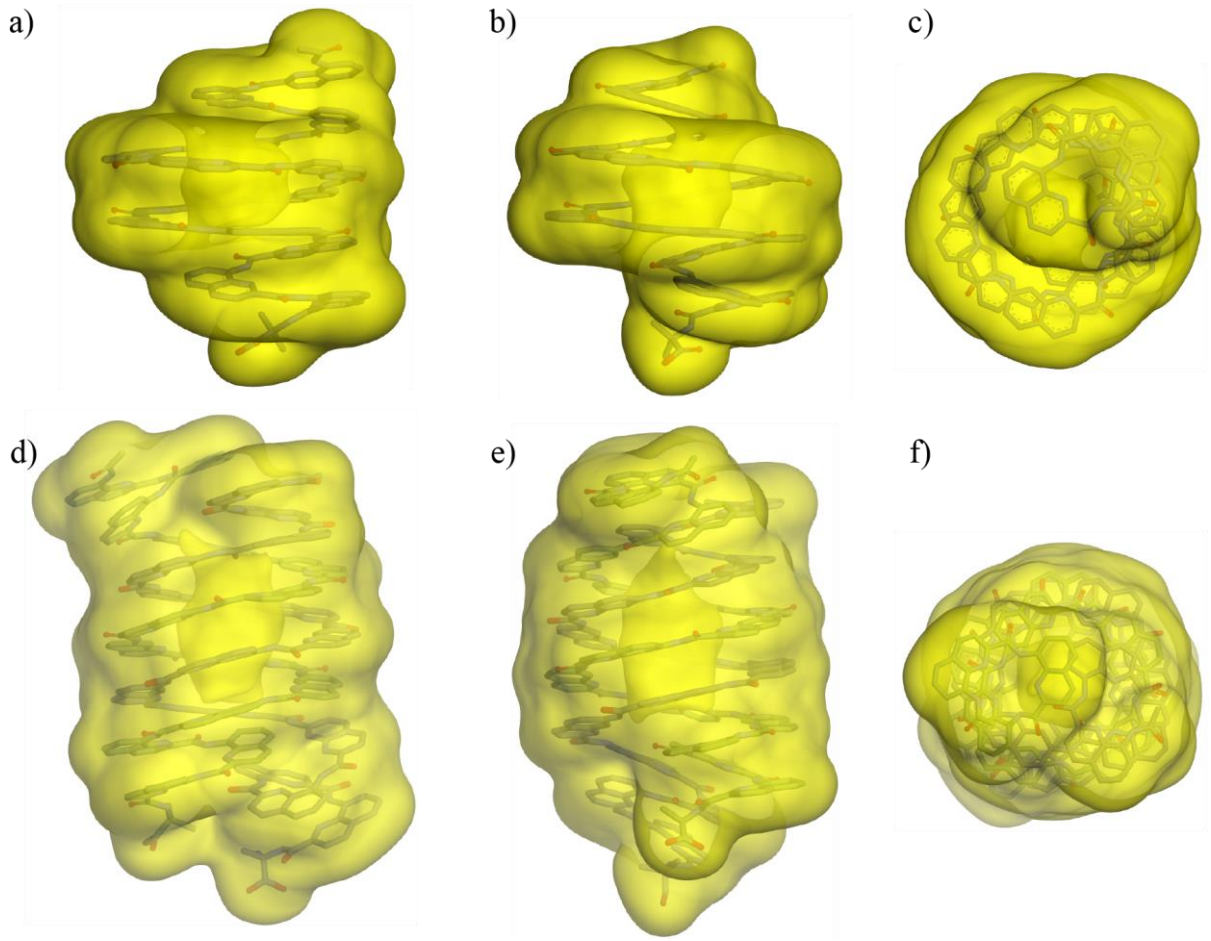

Figure S9. Solvent accessible surface of two conformations of 5: (a) front view, b) side view and c) top view of single helix **5**. Solvent accessible surface of: (d) front view, e) side view and f) top view of duplex $(\mathbf{5})_2$. All solvent accessible surfaces are shown as transparent yellow isosurfaces. Solvent-accessible surface area was calculated by discovery studio software rolling ball method with a radius of 1.4 Å. The solvent accessible surface was predicted to be 2690 $Å^2$ for the double helix state and 1790 $Å^2$ for the single helix. Side chains have been removed for the surface estimation.

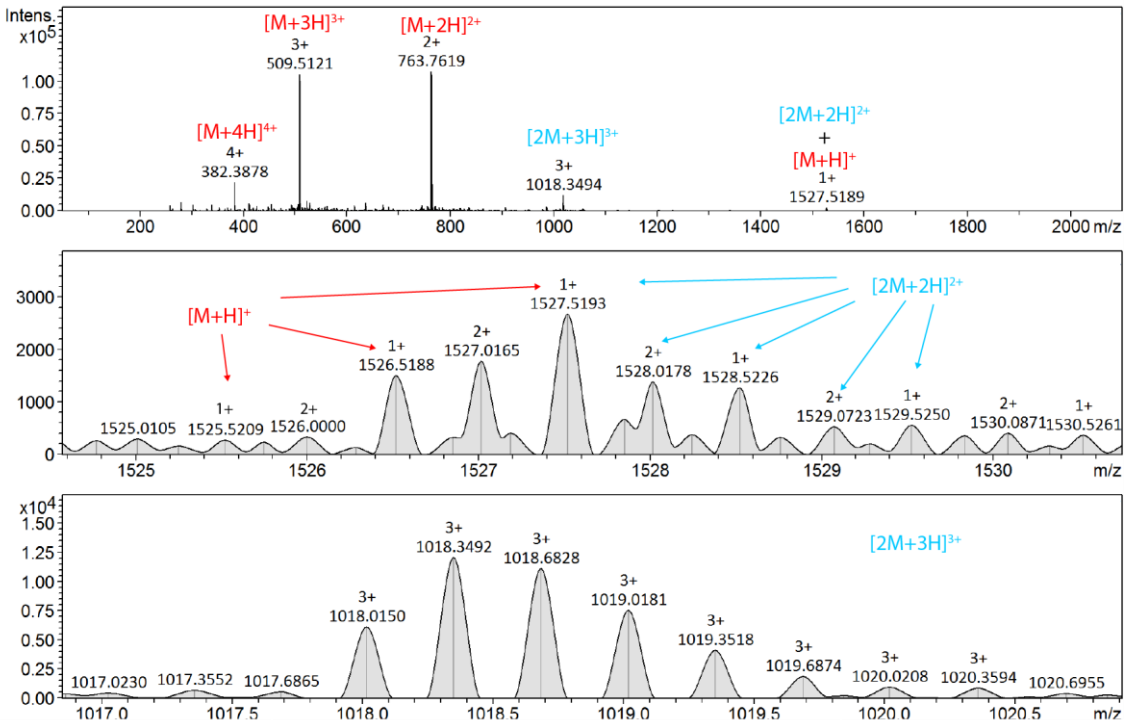

Figure S10. ESI-MS spectrum of oligomer 6 (direct infusion of an aqueous sample). Peaks corresponding to monomeric and dimeric species are highlighted in red and blue, respectively. The $[M+H]^+$ peak is superimposed by the $[2M+2H]^{2+}$ peak, while the mass envelope suggests a major population of the $[2M+2H]^{2+}$ species.

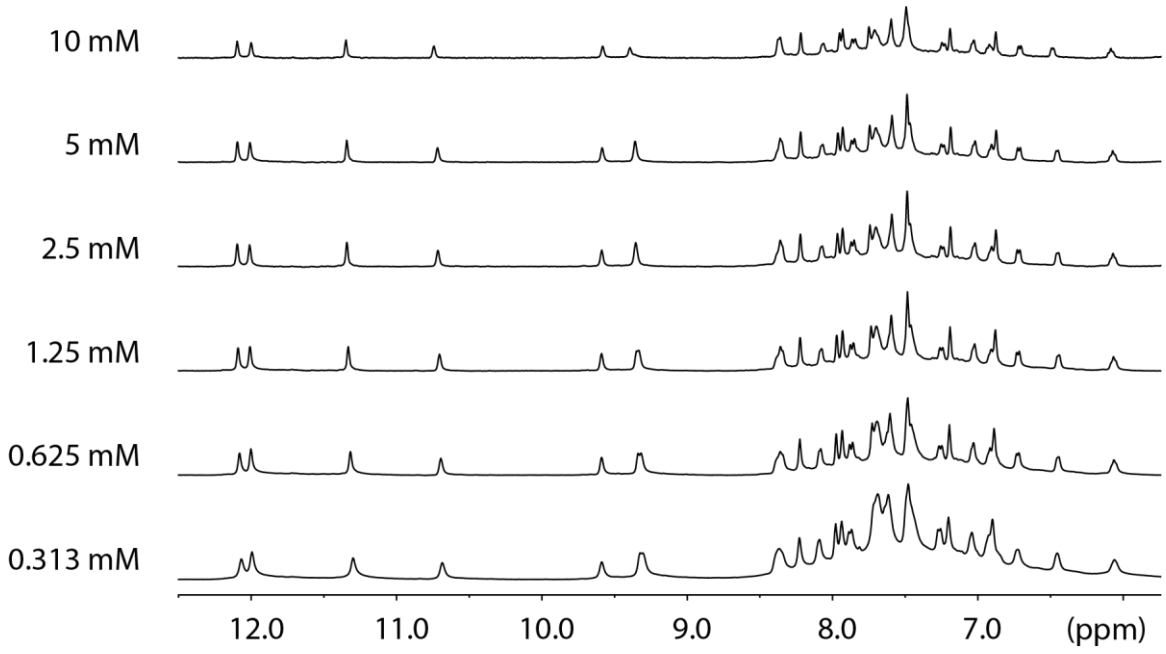

Figure S11. Variable concentration ^{1}H NMR spectra of oligomer 6. The spectra were recorded with water suppression (500 MHz, H_2O/D_2O (9:1, *v*/*v*), 25 °C).

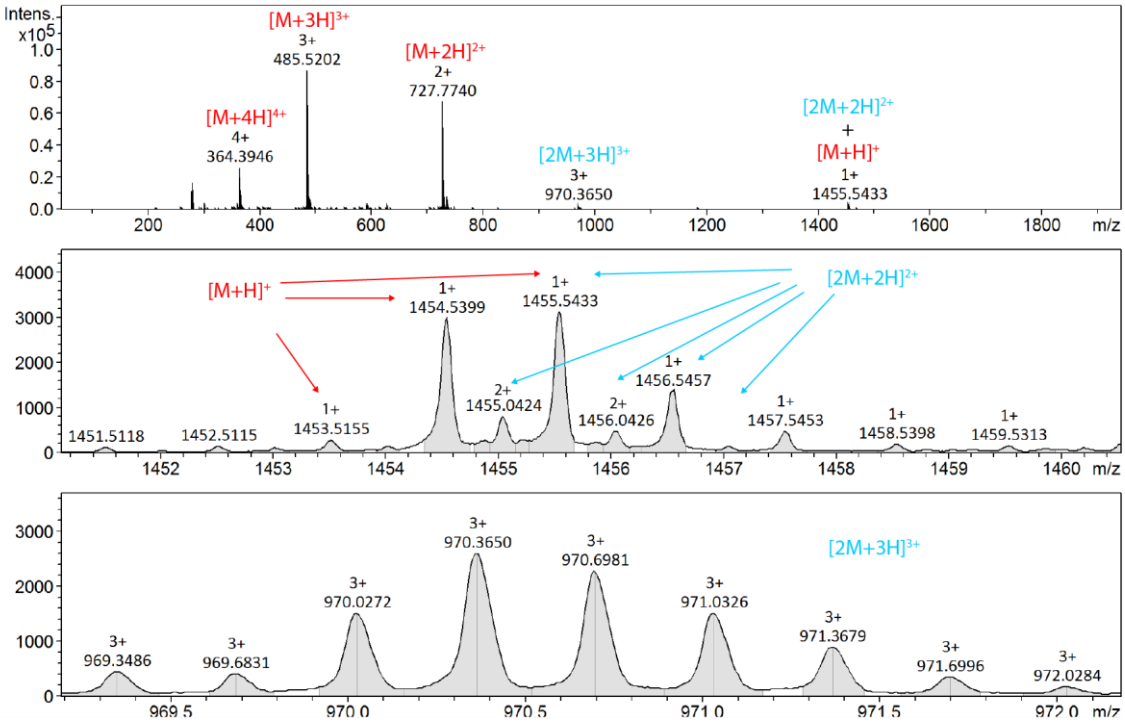

Figure S12. ESI-MS spectrum of oligomer 7 (direct infusion of an aqueous sample). Peaks corresponding to monomeric and dimeric species are highlighted in red and blue, respectively. The $[M+H]^+$ peak is superimposed by the $[2M+2H]^{2+}$ peak.

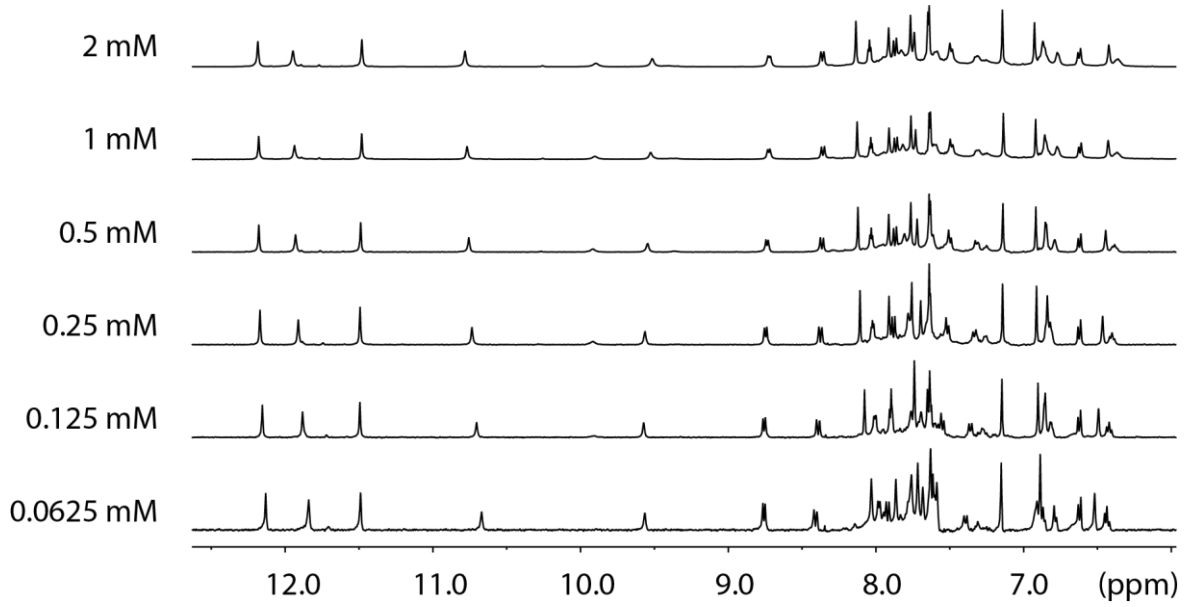

Figure S13. Variable concentration ^{1}H NMR spectra of oligomer 7. The spectra were recorded with water suppression (500 MHz, H_2O/D_2O (9:1, *v*/*v*), 25 °C).

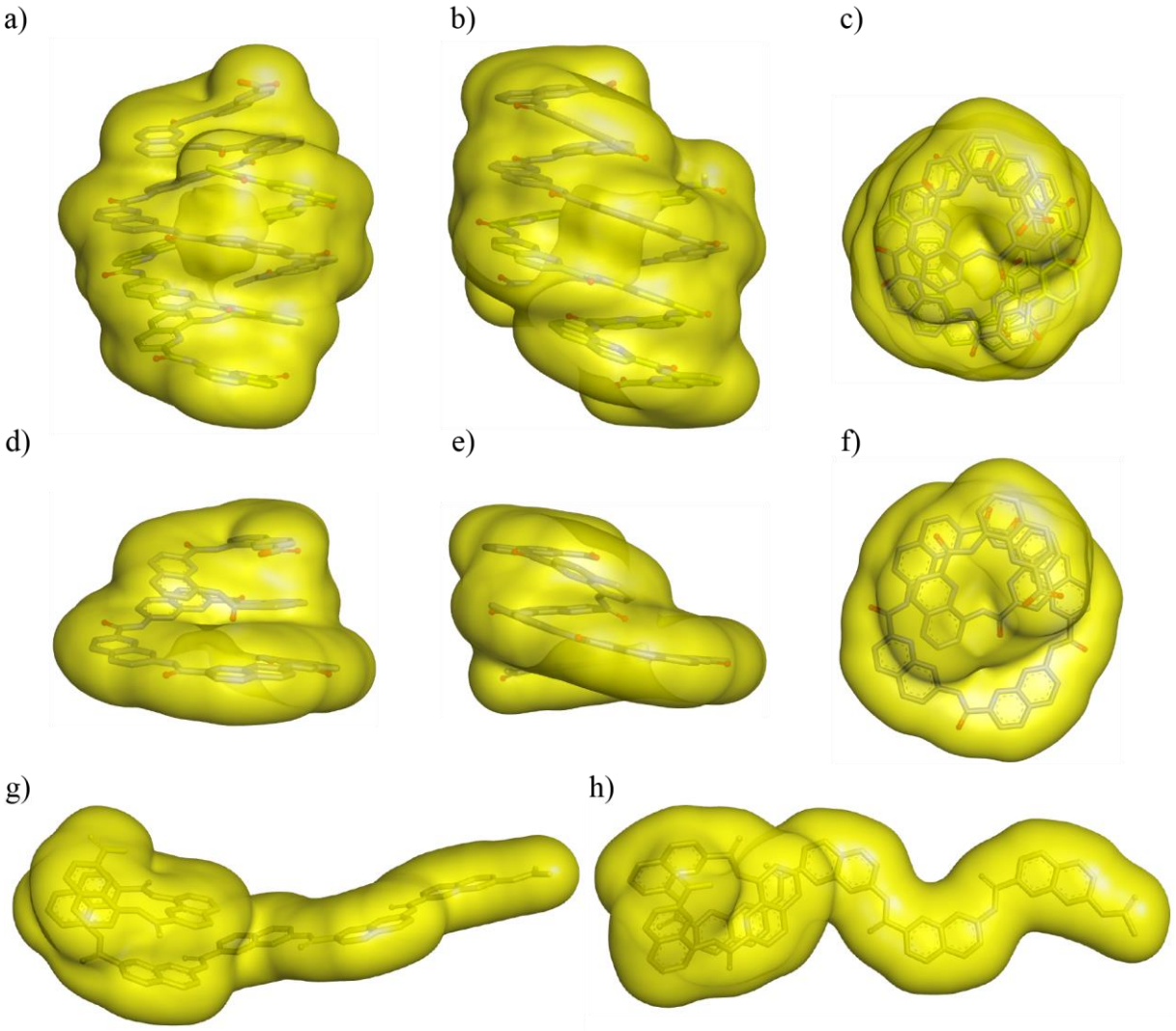

Figure S14. Solvent accessible surface of three conformations of oligomer 7: (a) front view, b) side view and c) top view of duplex $(\mathbf{7})_2$. Solvent accessible surface of: d) front view, e) side view and f) top view of single helix **7**. Solvent accessible surface of: g) front view and h) top view of extended state **7**. All solvent accessible surfaces are shown as transparent yellow isosurfaces. Solvent-accessible surface area was calculated by discovery studio software rolling ball method with a radius of 1.4 Å. The solvent accessible surface was predicted to be 1680 $Å^2$ for the double helix state, 1380 $Å^2$ for the extended monomer and 1160 $Å^2$ for the single helix. Thus, it can be estimated that the double helix form exposes to the solvent only around 61% or 71% of the area exposed by two individual monomeric species. Side chains have been removed for the surface estimation.

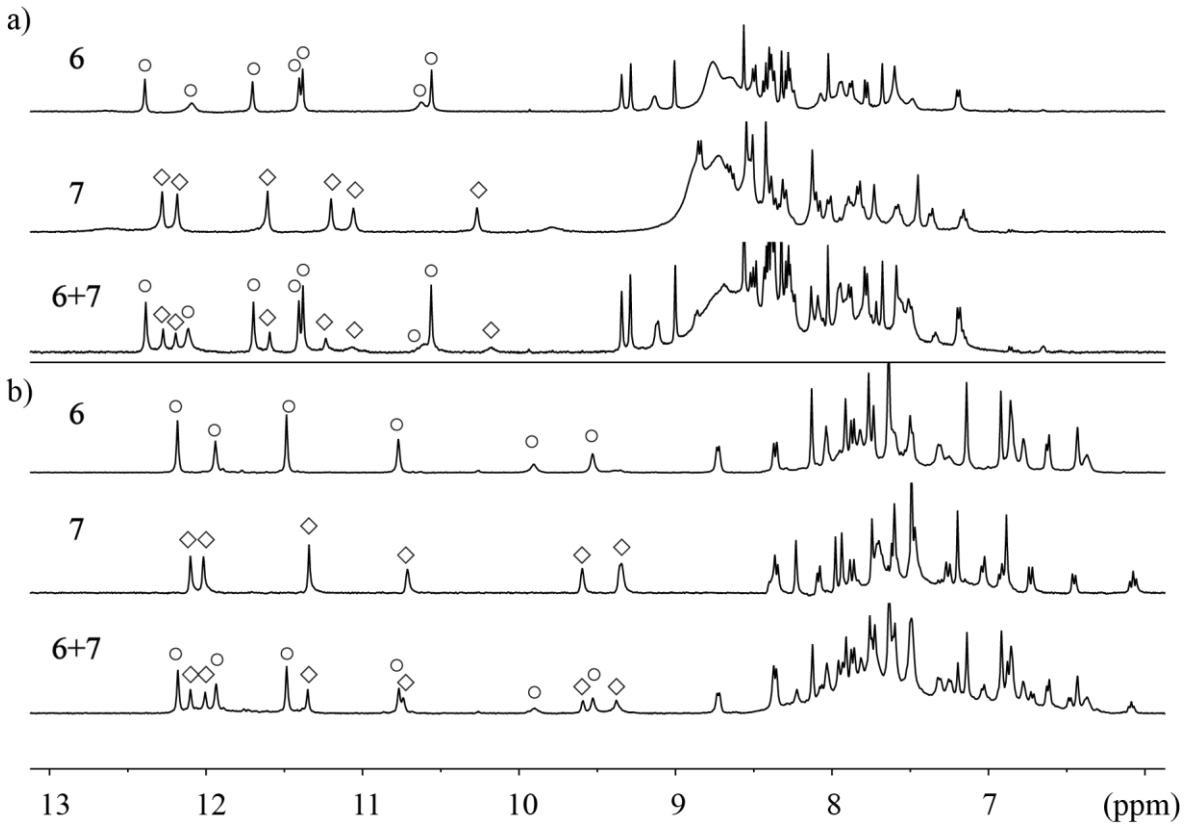

Figure S15. Hybridization experiments of 6 and 7. Excerpts of ^{1}H NMR (500 MHz, water suppression) at 25 °C of oligomer **6**, oligomer **7**, and the mixture of two oligomers at 0.5 mM in a) DMSO-d_6 and b) H_2O/D_2O (9:1, *v*/*v*). Signals corresponding to oligomer **6** and **7** are marked in circles and diamonds, respectively.

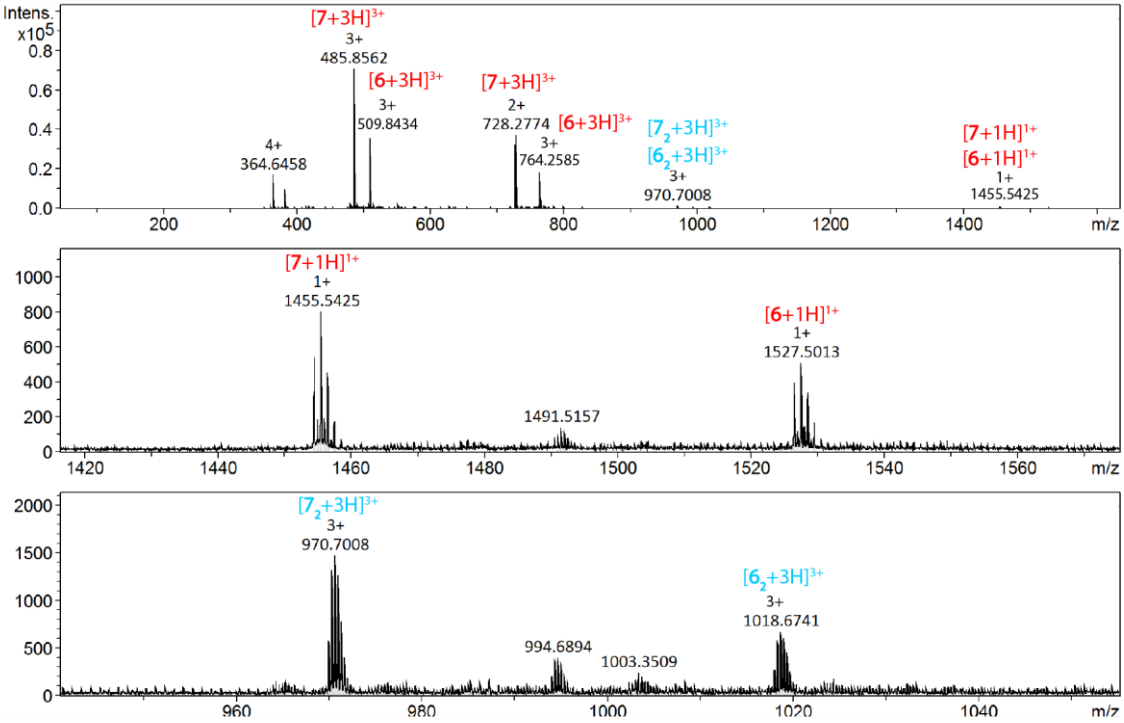

Figure S16. ESI-MS spectrum of oligomer 6 and 7 mixture (direct infusion of an aqueous sample). Peaks corresponding to monomeric and dimeric species are highlighted in red and blue, respectively.

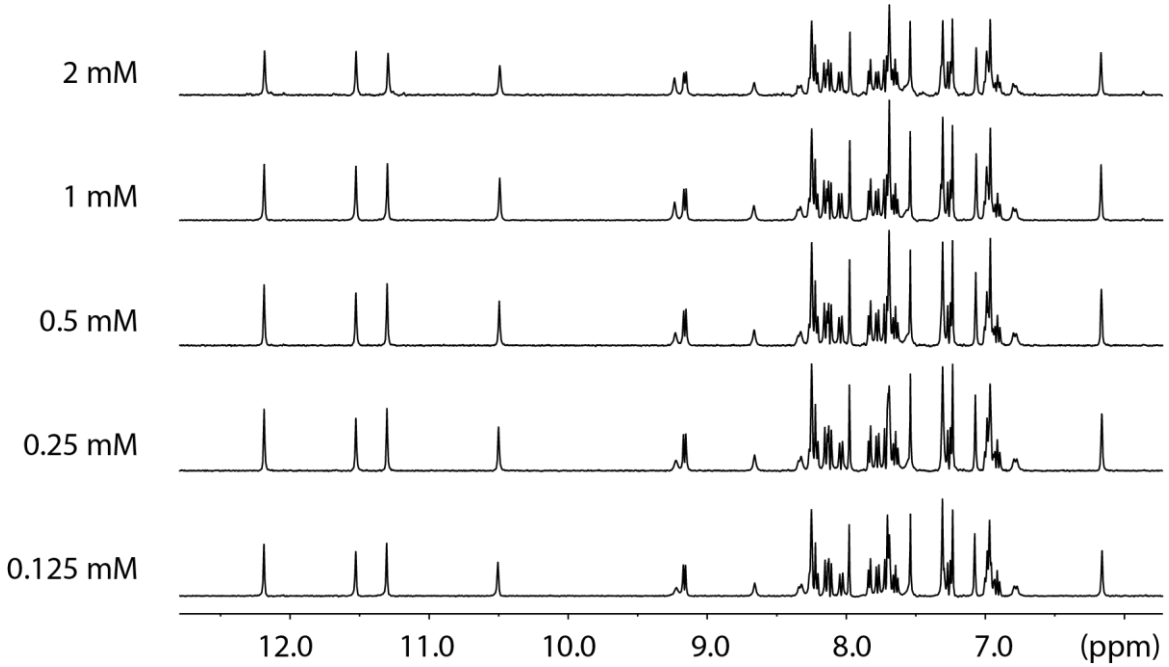

Figure S17. Variable concentration ^{1}H NMR spectra of oligomer 8. The spectra were recorded with water suppression (500 MHz) in 12 mM ammonium acetate aqueous buffer pH 8.5 at 25 °C.

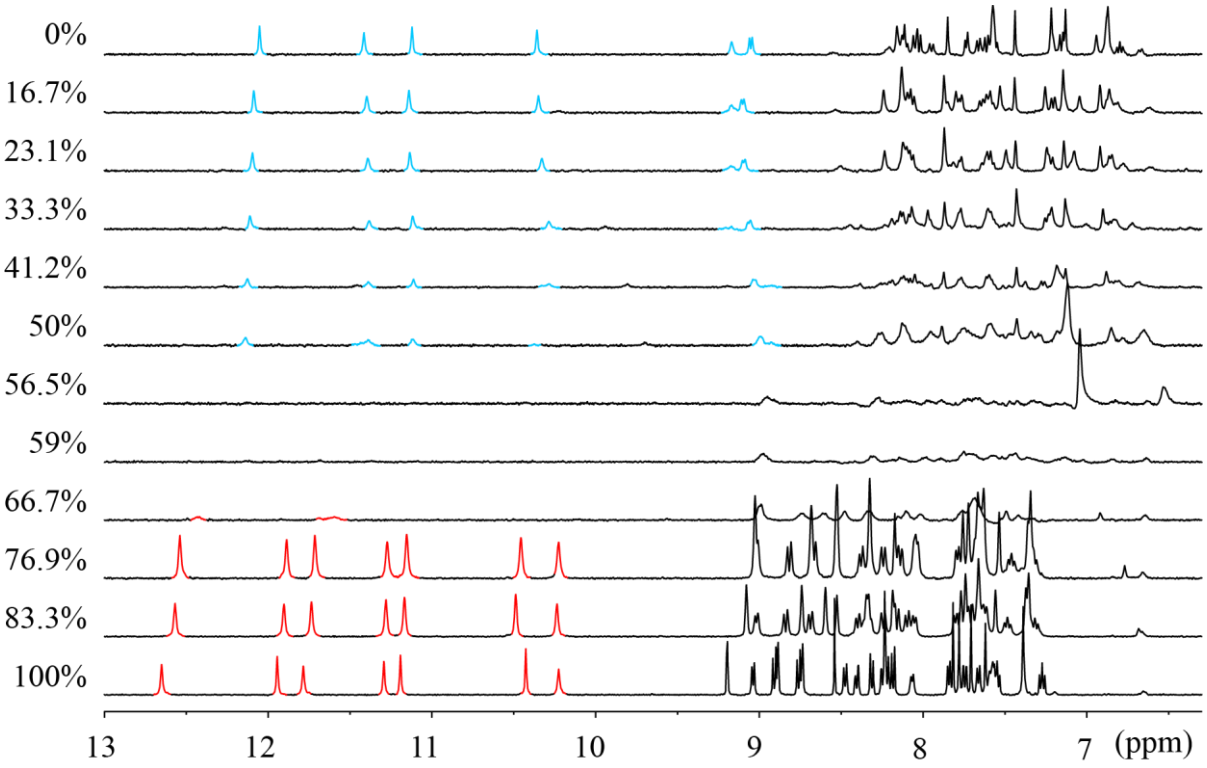

Figure S18. DMSO-d_6/H_2O variation ^{1}H NMR spectra of 8. ^{1}H NMR (500 MHz) spectra at 25 °C of oligomer **8** in DMSO-d_6/H_2O mixtures with different DMSO contents. Signals corresponding to monomeric and dimeric species are highlighted in red and blue, respectively. Note: 0% DMSO means ^{1}H NMR (500 MHz) spectra of oligomer **8** in H_2O/D_2O (9:1, *v*/*v*).

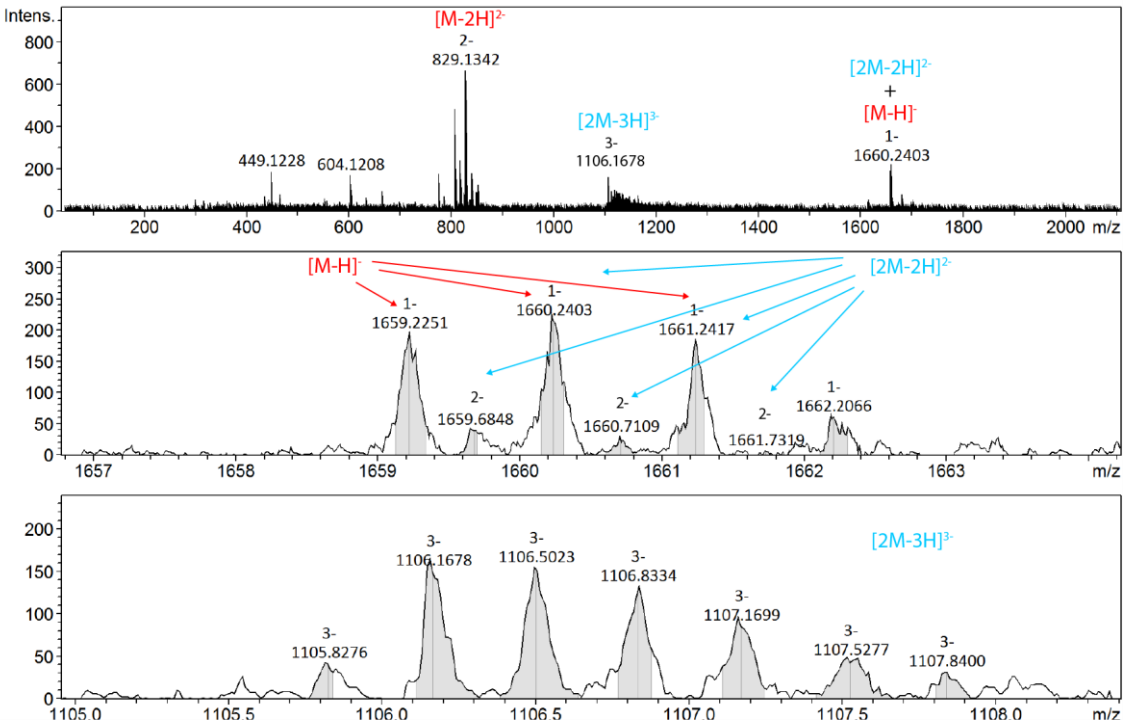

Figure S19. ESI-MS spectrum of oligomer 8 (direct infusion of an aqueous sample). Peaks corresponding to monomeric and dimeric species are highlighted in red and blue, respectively. The $[M-H]^-$ peak is superimposed by the $[2M-2H]^{2-}$ peak.

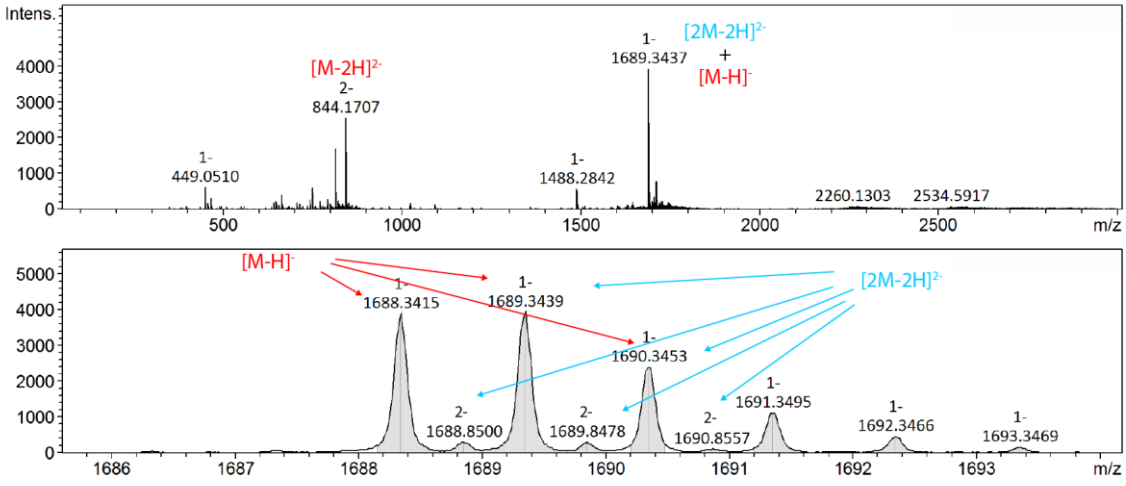

Figure S20. ESI-MS spectrum of oligomer 9 (direct infusion of an aqueous sample). Peaks corresponding to monomeric and dimeric species are highlighted in red and blue, respectively. The $[M-H]^-$ peak is superimposed by the $[2M-2H]^{2-}$ peak.

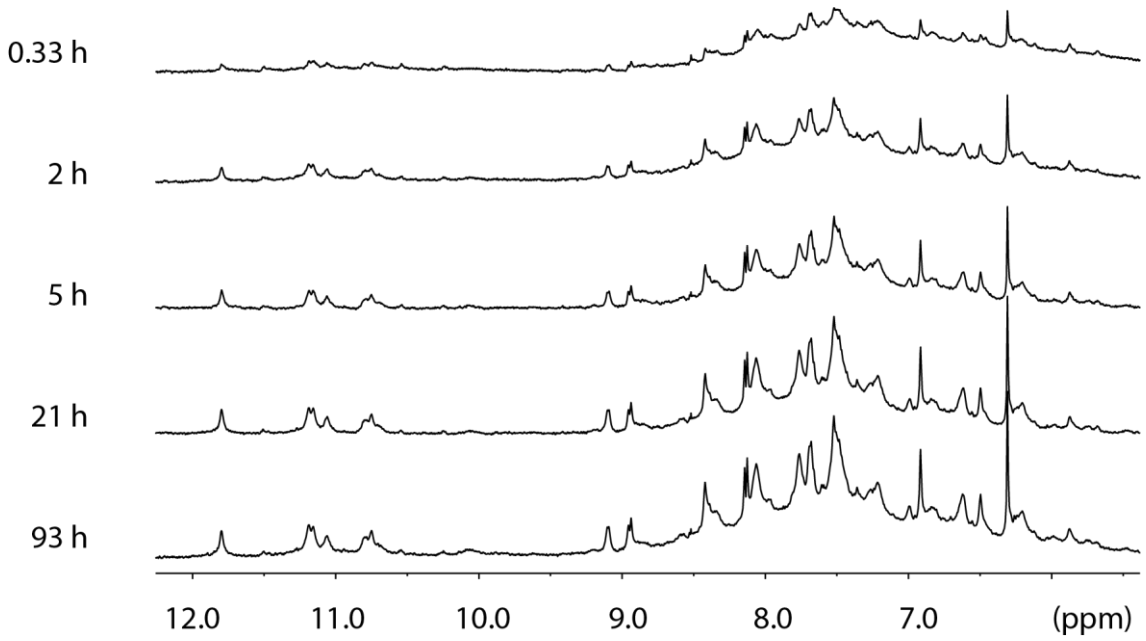

Figure S21. Variable incubation time ^{1}H NMR spectra of 9 in buffer solution. Excerpts of ^{1}H NMR (500 MHz, water suppression) at 25 °C of oligomer **9** at 5 mM in 48 mM ammonium acetate aqueous buffer pH 8.5 in the different incubation times.

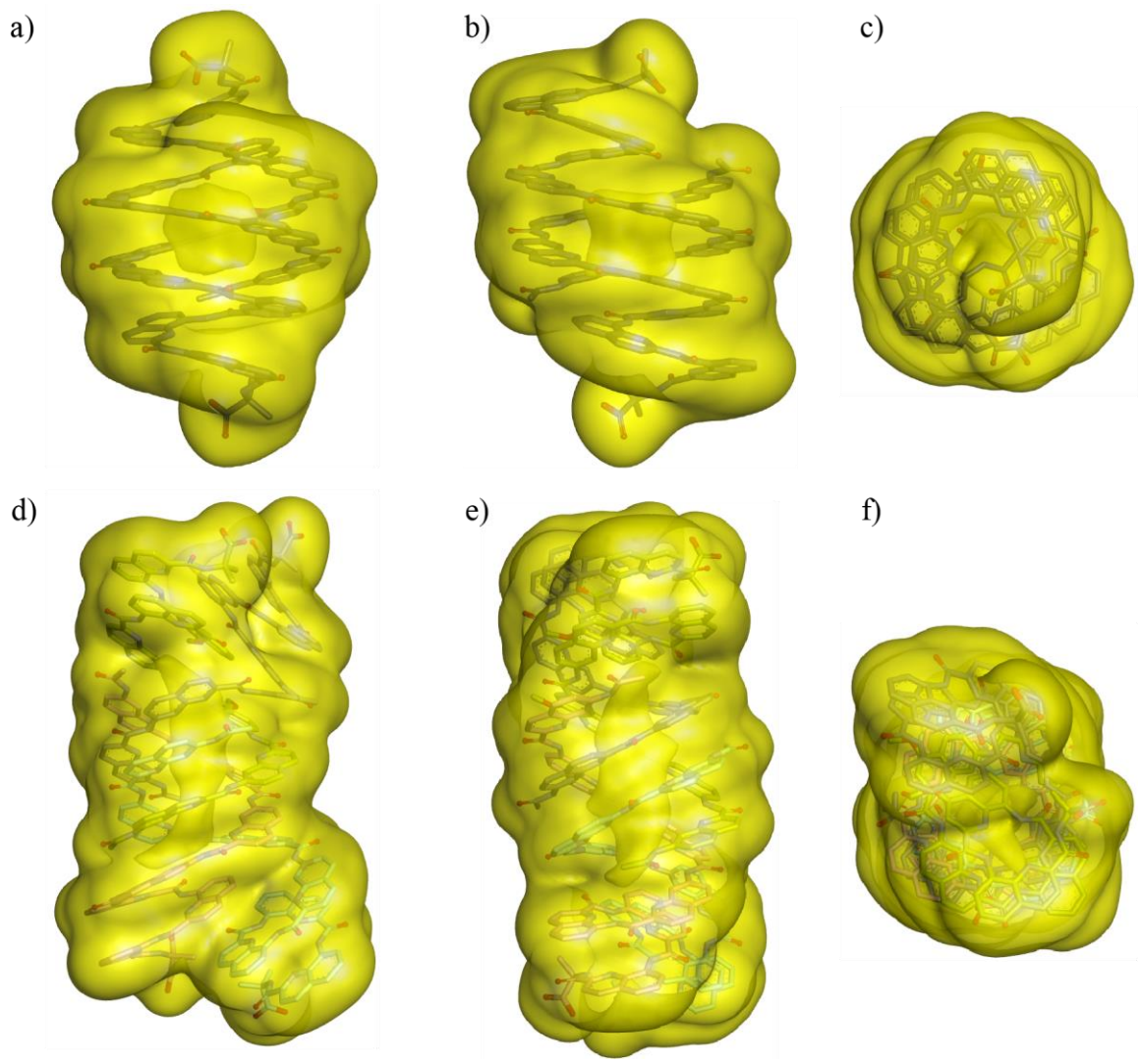

Figure S22. Solvent accessible surface of two conformations of 9: (a) front view, b) side view and c) top view of duplex (**9**)$_2$. Solvent accessible surface of: d) front view, e) side view and f) top view of tetrameric helix (**9**)$_4$. All solvent accessible surfaces are shown as transparent yellow isosurfaces. Solvent-accessible surface area was calculated by discovery studio software rolling ball method with a radius of 1.4 Å. The solvent accessible surface was predicted to be 3210 Å^2 for the tetra helix state and 1810 Å^2 for the double helix state. Thus, it can be estimated that the tetra helix form exposes to the solvent only around 89% of the area exposed by two individual double species.

2 Materials and Methods

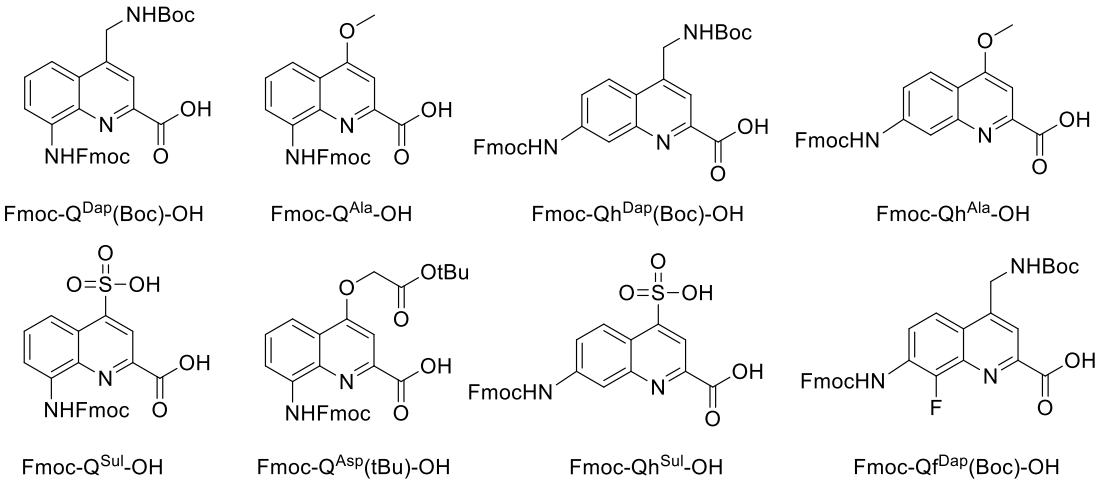

Figure S23. Protected Fmoc-acid building blocks used in this study. Fmoc-Q^{Dap}(Boc)-OH[1], Fmoc-Q^{Ala}-OH[2], Fmoc-Q^{Sul}-OH[3], Fmoc-Q^{Asp}(*t*Bu)-OH[4], Fmoc-Qh^{Dap}(Boc)-OH[1] and Fmoc-Qf^{Dap}(Boc)-OH[1] have been described previously. For detailed synthetic procedures to prepare Fmoc-Qh^{Ala}-OH and Fmoc-Qh^{Sul}-OH, see section 2.3.

2.1 General

General. Commercial reagents (Suppliers: Abcr, Fisher Scientific, Merck, Sigma-Aldrich, TCI, BLDpharm or VWR) were used without further purification unless otherwise stated. LL Wang resin (100–200 mesh) was purchased from Sigma-Aldrich. Cl-MPA protide resin was purchased from CEM. Peptide grade *N*,*N*-dimethylformamide (DMF) was purchased from Carlo Erba. Anhydrous chloroform, triethylamine (TEA) and *N*,*N*-diisopropylethylamine (DIEA) were obtained via distillation over CaH_2 prior to use. Anhydrous tetrahydrofuran (THF) and dichloromethane (DCM) were obtained via an MBRAUN SPS-800 solvent purification system. Ultrapure water was obtained via a Sartorius arium® pro VF ultrapure water system. Reactions were monitored by thin layer chromatography (TLC) on Merck silica gel 60-F254 plates and observed under UV light. Column chromatography purifications were carried out on Merck GEDURAN Si60 (40–63 µm). Nuclear magnetic resonance (NMR) spectra were recorded on an Avance III HD 400 MHz Bruker BioSpin spectrometer or an Avance III HD 500 MHz Bruker BioSpin spectrometer equipped with a broad band observe 5-mm BB-H&FD CryoProbe™ Prodigy. Measurements were performed at 25 °C unless stated otherwise. Water suppression was performed with excitation sculpting method. Processing was done with MestReNova (v.12.0.0-20080) NMR processing software from Mestrelab Research. Chemical

shifts are reported in ppm and calibrated via residual solvent signals or 3-(trimethylsilyl)propionic-2,2,3,3-d_4 acid sodium salt (TMSP) when water suppression was applied. Signal multiplicities are abbreviated as s, singlet; d, doublet; t, triplet; q, quartet, and m, multiplet. Signals were assigned using ^{1}H-^{13}C HMQC and ^{1}H-^{13}C HMBC spectra. Electrospray ionization (ESI) mass spectra were recorded on Bruker microTOF II and Thermo Finnigan LTQ FT Ultra spectrometers. Electron ionization (EI) mass spectra were recorded on a Thermo Q Exactive GC Orbitrap or a Finnigan MAT 95 sector mass spectrometer. Analytical and semi-preparative reversed phase (RP) high performance liquid chromatography (HPLC) were performed on a Thermo Fisher Scientific Ultimate 3000 HPLC System using Macherey-Nagel Nucleodur C18 Gravity columns (4 × 100 mm, 5 µm and 10 × 250 mm, 5 µm) or Macherey-Nagel Nucleodur C8 Gravity columns (4 × 50 mm, 5 µm and 10 × 100 mm, 5 µm) with different gradients of 0.1% TFA water and 0.1% TFA acetonitrile. All ultraviolet–visible (UV/Vis) absorbance measurements were done with a Jasco V-750 spectrophotometer instrument using a 1 cm quartz cuvette. Measurements were performed at 20 °C if not stated otherwise. Microwave-assisted solid phase foldamer synthesis (SPFS) was performed with a CEM® Discover Bio manual microwave apparatus. The temperature within the reactor vessel was monitored with an optical fiber probe. Automated SPFS was done on a PurePep® Chorus synthesizer (Gyros Protein Technologies) by applying induction heating. The DOSY spectra were recorded on a Avance III HD 500 MHz Bruker BioSpin spectrometer equipped with a broad band observe 5-mm BB-H&FD CryProbe™ Prodigy with a pulse sequence with stimulated echo using bipolar gradient pulses for diffusion and a 3-9-19 watergate solvent suppression pulse sequence from the Bruker pulse program library (stebpgp1s19). The diffusion delay Δ (big delta) was set to 175 ms and the diffusion gradient pulse length δ (little delta) was set to 1.1 ms. The number of gradient steps were set to 32 with linear spacing starting from 2% reaching 95% of the full gradient strength in the final step. For each of the 32 gradient amplitudes, 128 transients of 32k complex data points were acquired. DOSY processing was performed with the DOSY processing tool from MestReNova (v.12.0.0-20080).

2.2 Solid phase synthesis procedures

Some oligomers were synthesized according to previously reported SPFS protocols,[5] hereafter referred to as manual synthesis method. Of note, in the case of Q^{Sul} and Qh^{Sul}-containing sequences, 2% DBU in NMP was employed for Fmoc deprotection, thus avoiding the additional washing steps with 20% DIEA in NMP like previously reported.[5] Other oligomers were prepared using the automated foldamer solid phase synthesis protocols recently reported.[6]

Final acetylation of the N-terminal aromatic amine: H_2N-$(Q)_n$-Wang resin and DIEA (6.0 equiv.) were suspended in anhydrous THF (1.25 mL) then acetyl chloride (4.0 equiv.) in anhydrous THF (1.25 mL) was added. The reaction vessel was then placed under microwave irradiation (25 W, ramp to 50 °C over 5 min, then hold at 50 °C for 15 min). The resin was filtered off and washed with anhydrous THF (2 × 3 mL). This acetylation step was repeated once using the same conditions.

Resin cleavage: The resin-bound foldamer was placed in a syringe equipped with a filter, washed with DMF (3 × 3 mL) and DCM (3 × 3 mL), and dried by passing N_2 flow through it. It was then suspended in a solution of TFA/*i*Pr_3SiH/H_2O (95:2.5:2.5, *v*/*v*/*v*). The resin was next gently shaken for at least 2 h at room temperature, then filtered off and rinsed one time with TFA. The foldamer was precipitated from the TFA cleavage solution by adding cold Et_2O and centrifugation to obtain a crude precipitate.

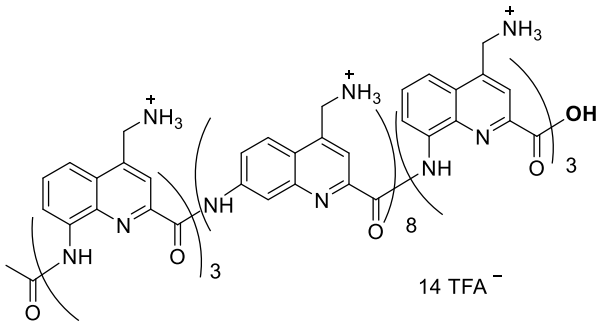

Oligomer 1: The synthesis of this oligomer has already been published.[1]

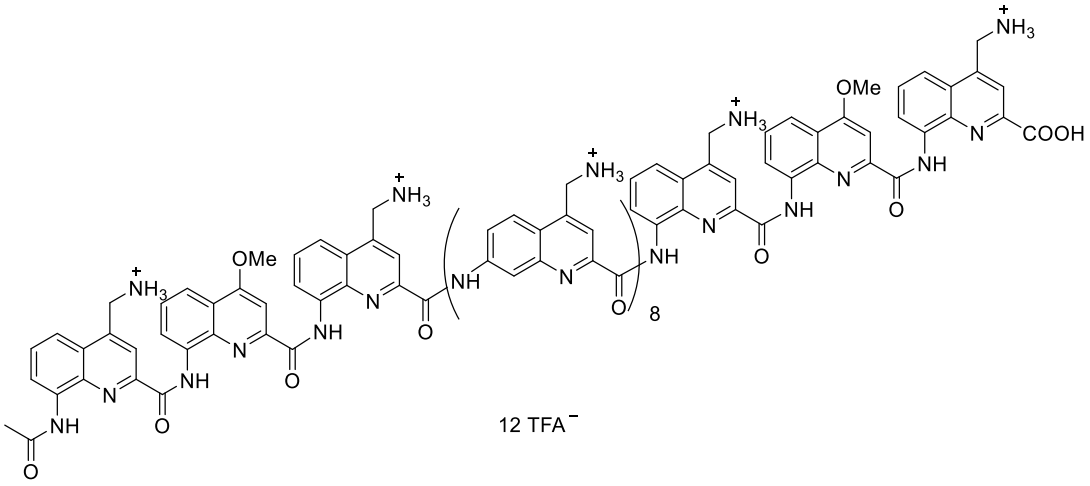

Oligomer 2: Oligomer **2** was synthesized starting from LL-Wang resin (0.37 mmol g^{-1}, 25 µmol scale) according to the manual synthesis method. Loading of the first monomer: 0.25 mmol g^{-1}

(70%). Final acetylation was carried out via the general acetylation method. After precipitation in cold Et_2O, the crude mixture was purified by semi prep RP-HPLC to give the **2** as a yellow solid (48 mg, 45%).

^{1}H NMR (500 MHz, H_2O/D_2O (9:1, *v*/*v*)) δ 12.11 (s, 1H), 12.03 (s, 1H), 12.01 (s, 1H), 11.56 (s, 1H), 11.33 (s, 1H), 10.72 (s, 1H), 10.54 (s, 1H), 10.37 (s, 1H), 10.20 (s, 1H), 10.03 (s, 1H), 10.00 (s, 1H), 9.54 (s, 1H), 9.47 (s, 1H), 9.38 (s, 1H), 9.34 (s, 1H), 8.82 – 8.71 (m, 2H), 8.61 (d, *J* = 10.7 Hz, 1H), 8.52 (d, *J* = 11.9 Hz, 2H), 8.39 – 7.99 (m, 18H), 7.99 – 7.71 (m, 13H), 7.71 – 7.52 (m, 12H), 7.52 – 7.07 (m, 26H), 7.07 – 6.85 (m, 12H), 6.84 – 6.57 (m, 6H), 6.56 – 6.27 (m, 6H), 3.53 (s, 3H), 3.21 (s, 3H).
HRMS: calcd. for $C_{156}H_{129}N_{40}O_{18}$ $[M+H]^+$ 2850.0403; found 2849.9474.

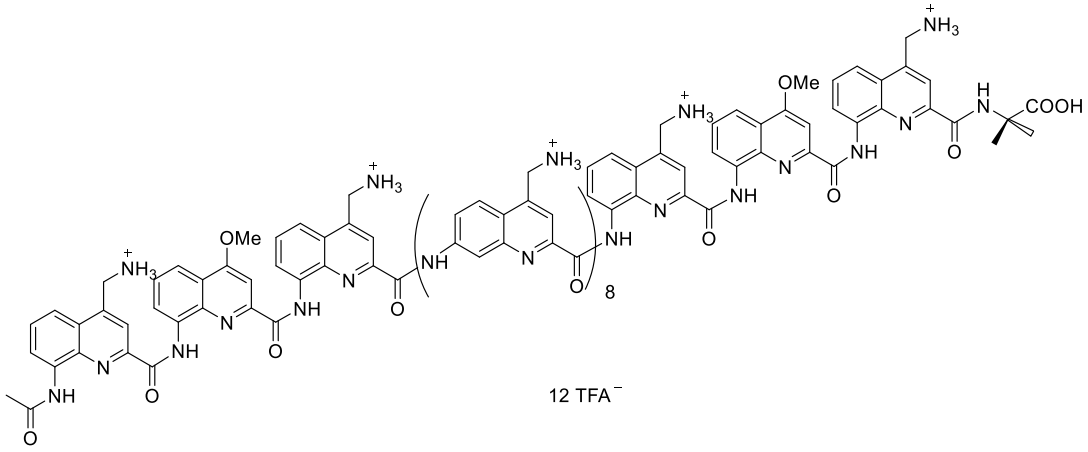

Oligomer 3: Oligomer **3** was synthesized starting from LL-Wang resin (0.37 mmol g^{-1}, 23 µmol scale) according to the automated synthesis method. Loading of the first monomer: 0.26 mmol g^{-1} (70%). Final acetylation was carried out via the general acetylation method. After precipitation in cold Et_2O, the crude mixture was purified by semi prep RP-HPLC to give the **3** as a yellow solid (56 mg, 56%).

^{1}H NMR (500 MHz, H_2O/D_2O (9:1, *v*/*v*)) δ 12.07 (s, 1H), 12.03 (s, 2H), 11.47 (s, 1H), 11.10 (s, 1H), 10.72 (s, 1H), 10.50 (s, 1H), 10.41 (s, 1H), 10.28 (s, 1H), 10.03 (s, 1H), 9.84 (s, 1H), 9.68 (s, 1H), 9.47 (s, 1H), 9.36 (s, 1H), 8.77 (d, *J* = 10.7 Hz, 1H), 8.74 – 8.63 (m, 2H), 8.53 (d, *J* = 10.6 Hz, 1H), 8.46 (d, *J* = 10.1 Hz, 1H), 8.37 (s, 1H), 8.34 – 8.14 (m, 8H), 8.10 – 7.99 (m, 5H), 7.98 – 7.58 (m, 16H), 7.58 – 6.85 (m, 27H), 6.74 – 6.44 (m, 7H), 6.33 (d, *J* = 9.0 Hz, 1H), 3.49 (s, 3H), 3.22 (s, 3H), 1.32 (s, 3H), 0.72 (s, 3H), 0.45 (s, 3H).
HRMS: calcd. for $C_{160}H_{137}N_{41}O_{19}$ $[M+2H]^{2+}$ 1468.0502; found 1468.1223.

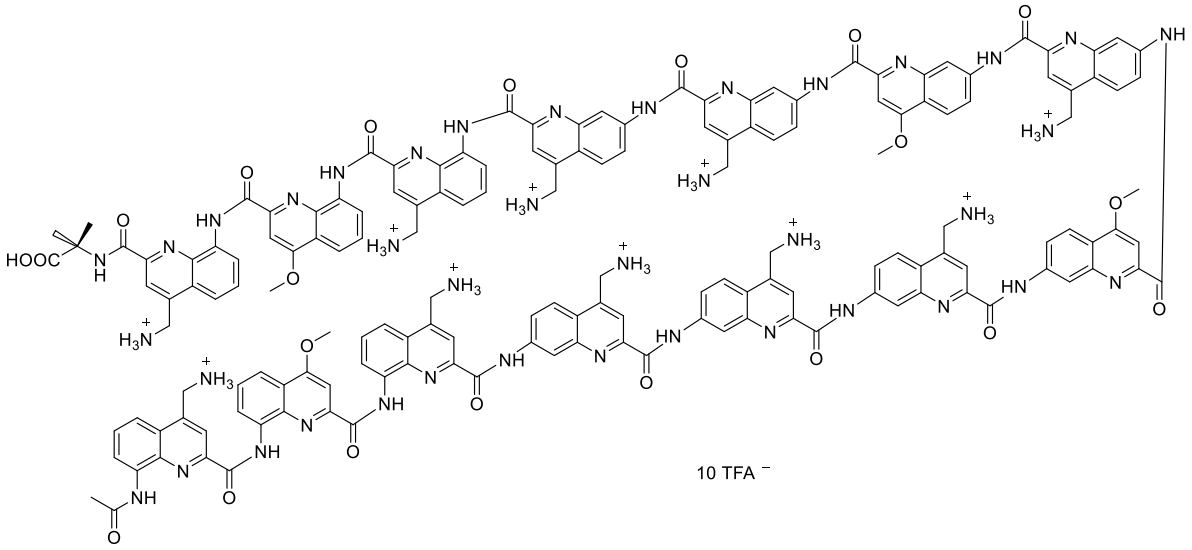

Oligomer 4: Oligomer **4** was synthesized starting from LL-Wang resin (0.37 mmol g^{-1}, 29 µmol scale) according to the manual synthesis method. Loading of the first monomer: 0.28 mmol g^{-1} (76%). Final acetylation was carried out via the general acetylation method. After precipitation in cold Et_2O, the crude mixture was purified by semi prep RP-HPLC to give the **4** as a yellow solid (42 mg, 36%).

^{1}H NMR (500 MHz, H_2O/D_2O (9:1, *v*/*v*)) δ 11.70 (s, 1H), 11.22 (s, 1H), 10.89 (s, 1H), 10.55 (s, 1H), 10.48 (s, 1H), 10.43 (s, 1H), 10.19 (s, 1H), 9.65 (s, 1H), 9.50 (s, 1H), 9.10 (s, 1H), 8.65 (d, *J* = 7.8 Hz, 1H), 8.46 (s, 1H), 8.41 (d, *J* = 10.1 Hz, 1H), 8.31 (s, 1H), 8.29 – 8.06 (m, 7H), 7.89 (d, *J* = 9.7 Hz, 1H), 7.76 – 7.47 (m, 21H), 7.46 – 7.17 (m, 22H), 7.17 – 6.81 (m, 20H), 6.81 – 6.46 (m, 12H), 6.45 – 6.17 (m, 7H), 6.15 – 6.00 (m, 2H), 3.90 (s, 3H), 3.22 (s, 3H), 3.04 (s, 3H), 1.82 (s, 3H).

HRMS: calcd. for $C_{160}H_{135}N_{39}O_{21}$ $[M+2H]^{2+}$ 1469.0342; found 1469.0595.

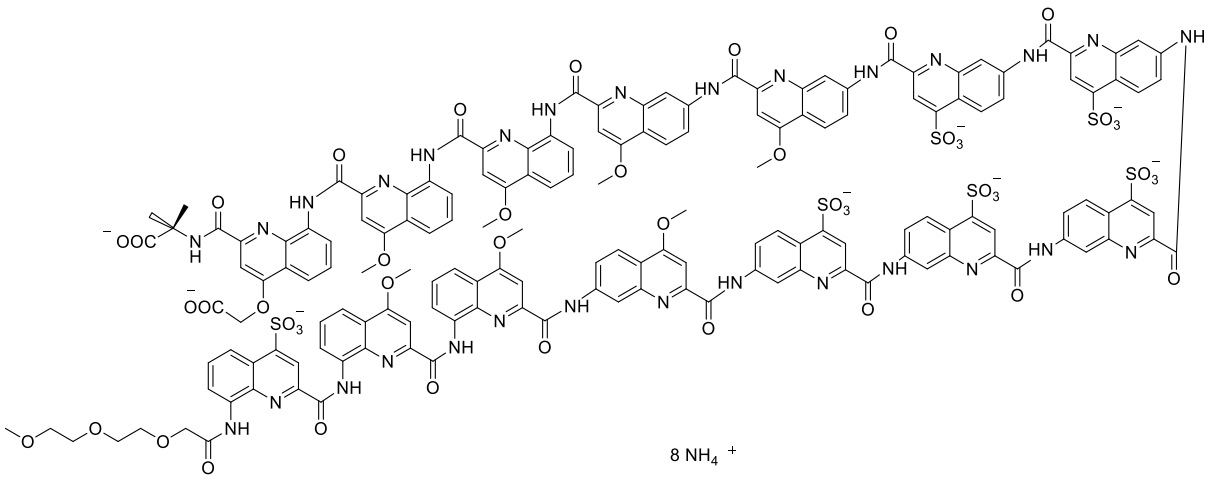

Oligomer 5: Oligomer **5** was synthesized starting from Cl-MPA-Protide resin (0.15 mmol g^{-1}, 20 µmol scale) according to the manual synthesis method. Loading of the first monomer: 0.13

mmol g^{-1} (86%). After precipitation in cold Et_2O, the crude mixture was purified by semi prep RP-HPLC to give the **5** as a yellow solid (15 mg, 22%).

^{1}H NMR (500 MHz, ammonium acetate aqueous buffer pH 8.5/D_2O (9:1, *v*/*v*)) δ 11.85 (s, 1H), 11.70 (s, 1H), 11.56 (s, 1H), 11.37 (s, 1H), 10.48 (s, 1H), 10.33 (s, 1H), 9.92 (s, 1H), 9.66 (s, 1H), 9.52 (s, 1H), 9.28 (s, 1H), 9.04 (d, *J* = 9.7 Hz, 1H), 8.85 (d, *J* = 9.4 Hz, 1H), 8.74 (s, 1H), 8.70 – 7.75 (m, 29H), 7.69 (d, *J* = 8.7 Hz, 2H), 7.50 – 7.03 (m, 19H), 7.01 – 6.11 (m, 21H), 5.94 (s, 2H), 4.00 (s, 4H), 3.43 (s, 5H), 3.10 (m, 13H), 2.62 (s, 3H), 2.34 (d, *J* = 18.6 Hz, 8H), 1.21 (m, 16H), 0.75 (s, 6H).
HRMS: calcd. for $C_{160}H_{119}N_{29}O_{48}S_6$ $[M-2H]^{2-}$ 1702.8038; found 1702.7972.

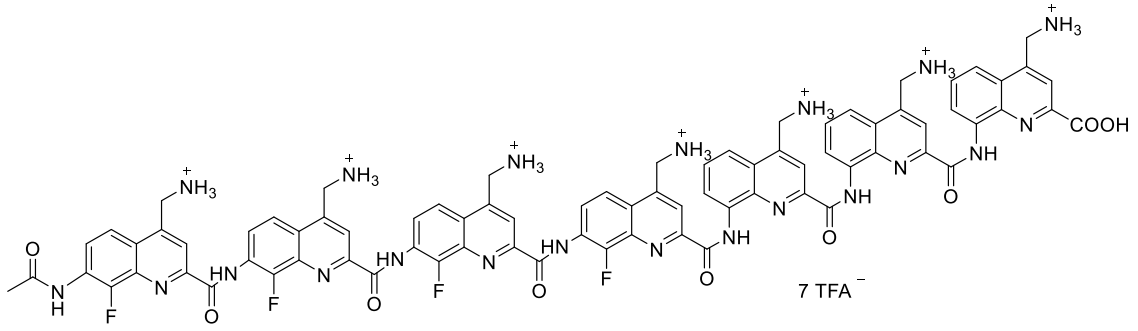

Oligomer 6: Oligomer **6** was synthesized starting from LL-Wang resin (0.44 mmol g^{-1}, 26 µmol scale) according to the manual synthesis method. Loading of the first monomer: 0.32 mmol g^{-1} (74%). Final acetylation was carried out via the general acetylation method. After precipitation in cold Et_2O to give the **6** as a grey solid (47 mg, 78%).

^{1}H NMR (400 MHz, H_2O/D_2O (9:1, *v*/*v*)) δ 12.10 (s, 1H), 12.02 (s, 1H), 11.34 (s, 1H), 10.71 (s, 1H), 9.60 (s, 1H), 9.35 (d, *J* = 5.5 Hz, 2H), 8.43 – 8.31 (m, 2H), 8.23 (s, 1H), 8.09 (d, *J* = 7.3 Hz, 1H), 7.98 (s, 1H), 7.94 (s, 1H), 7.89 (s, 1H), 7.86 (s, 1H), 7.77 – 7.63 (m, 6H), 7.63 – 7.54 (m, 3H), 7.53 – 7.40 (m, 7H), 7.26 (d, *J* = 9.8 Hz, 3H), 7.20 (s, 1H), 7.04 (d, *J* = 8.5 Hz, 2H), 6.96 – 6.80 (m, 3H), 6.73 (d, *J* = 9.0 Hz, 1H), 6.45 (d, *J* = 8.2 Hz, 1H), 6.08 (t, *J* = 8.3 Hz, 1H), 4.05 (m, 1H), 3.72 (d, *J* = 14.8 Hz, 1H), 3.47 (q, *J* = 7.3 Hz, 1H), 2.74 (d, *J* = 16.4 Hz, 1H), 1.75 (s, 3H).
HRMS: calcd. for $C_{79}H_{64}F_4N_{21}O_9$ $[M+H]^+$ 1526.5127; found 1526.5634.

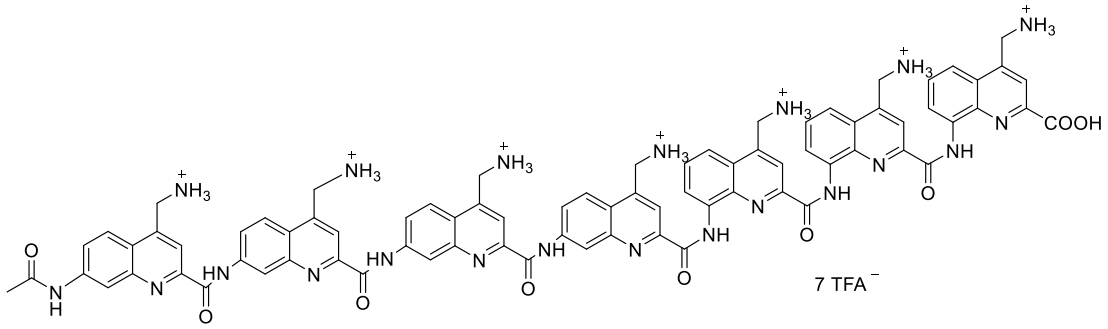

Oligomer 7: Oligomer **7** was synthesized starting from LL-Wang resin (0.44 mmol g^{-1}, 23 µmol scale) according to the manual synthesis method. Loading of the first monomer: 0.31 mmol g^{-1} (70%). Final acetylation was carried out via the general acetylation method. After precipitation in cold Et_2O to give the **7** as a grey solid (30 mg, 88%).

^{1}H NMR (500 MHz, H_2O/D_2O (9:1, *v*/*v*)) δ 12.18 (s, 1H), 11.94 (s, 1H), 11.49 (s, 1H), 10.77 (s, 1H), 9.91 (s, 1H), 9.53 (s, 1H), 8.73 (d, *J* = 8.1 Hz, 1H), 8.36 (d, *J* = 10.3 Hz, 1H), 8.13 (s, 2H), 8.04 (t, *J* = 4.5 Hz, 2H), 7.98 – 7.70 (m, 10H), 7.69 – 7.42 (m, 8H), 7.40 – 7.19 (m, 3H), 7.14 (s, 2H), 6.85 (m, 6H), 6.62 (d, *J* = 8.9 Hz, 2H), 6.43 (s, 1H), 6.37 (s, 1H).
HRMS: calcd. for $C_{79}H_{68}N_{21}O_9$ $[M+H]^+$ 1454.5503; found 1454.5802.

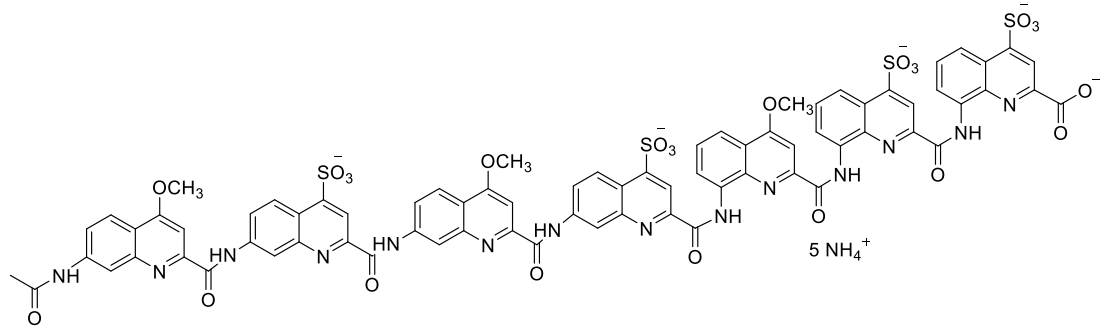

Oligomer 8: Oligomer **8** was synthesized starting from Cl-MPA-Protide resin (0.15 mmol g^{-1}, 20 µmol scale) according to the manual synthesis method. Loading of the first monomer: 0.14 mmol g^{-1} (90%). Final acetylation was carried out via the general acetylation method. After precipitation in cold Et_2O, the crude mixture was purified by semi prep RP-HPLC to give the **8** as a yellow solid (5 mg, 15%).

^{1}H NMR (500 MHz, ammonium acetate aqueous buffer pH 8.5/D_2O (9:1, *v*/*v*)) δ 12.19 (s, 1H), 11.53 (s, 1H), 11.30 (s, 1H), 10.49 (s, 1H), 9.23 (s, 1H), 9.16 (d, *J* = 8.5 Hz, 1H), 8.66 (s, 1H), 8.34 (d, *J* = 9.9 Hz, 1H), 8.29 – 8.02 (m, 6H), 7.97 (s, 1H), 7.87 – 7.61 (m, 6H), 7.54 (s, 1H), 7.34 – 7.22 (m, 4H), 7.07 (s, 1H), 7.03 – 6.87 (m, 3H), 6.79 (d, *J* = 10.9 Hz, 1H), 6.17 (s, 1H), 4.14 (s, 1H), 4.11 (s, 1H), 3.15 (s, 3H), 1.38 (s, 3H), 1.18 – 1.12 (m, 1H).

HRMS: calcd. for $C_{75}H_{51}N_{14}O_{24}S_4$ $[M-H]^-$ 1659.2078; found 1659.2261.

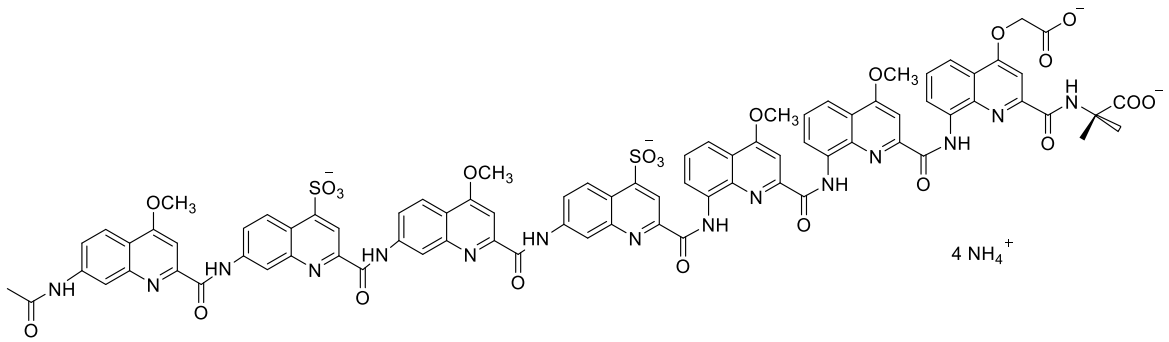

Oligomer 9: Oligomer **9** was synthesized starting from Cl-MPA-Protide resin (0.15 mmol g^{-1}, 18 µmol scale) according to the manual synthesis method. Loading of the first monomer: 0.11 mmol g^{-1} (75%). Final acetylation was carried out via the general acetylation method. After precipitation in cold Et_2O, the crude mixture was purified by semi prep RP-HPLC to give the **9** as a yellow solid (10 mg, 33%).

^{1}H NMR (500 MHz, ammonium acetate aqueous buffer pH 8.5/D_2O (9:1, *v*/*v*)) δ 11.53 (s, 1H), 10.72 (s, 1H), 10.55 (s, 1H), 10.28 (s, 1H), 9.40 (s, 1H), 9.27 (s, 1H), 9.25 (s, 1H), 8.94 (s, 2H), 8.80 (t, *J* = 12.3 Hz, 2H), 8.71 (d, *J* = 10.0 Hz, 1H), 8.60 – 8.51 (m, 2H), 8.37 (d, *J* = 10.8 Hz, 1H), 8.06 (s, 1H), 7.70 (s, 1H), 7.61 (t, *J* = 9.0 Hz, 2H), 7.54 (s, 1H), 7.39 (s, 1H), 7.31 – 7.17 (m, 3H), 6.90 (d, *J* = 8.3 Hz, 1H), 6.87 – 6.78 (m, 3H), 6.49 (s, 1H), 6.18 (d, *J* = 10.5 Hz, 1H), 6.13 (s, 1H), 5.90 (d, *J* = 7.3 Hz, 2H), 5.68 (s, 1H), 4.07 (s, 3H), 3.61 (s, 3H), 3.45 (d, *J* = 1.9 Hz, 3H), 3.12 (s, 3H), 2.32 (d, *J* = 2.0 Hz, 3H).
HRMS: calcd. for $C_{82}H_{62}N_{15}O_{23}S_2$ $[M-H]^-$ 1688.3579; found 1688.3416.

2.3 Monomer synthesis procedures

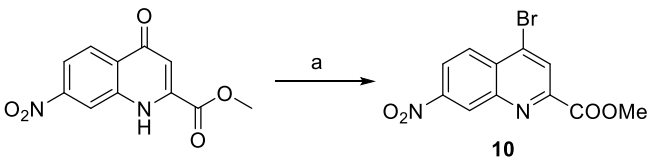

10

Compound 10. Methyl 7-nitro-4-oxo-1,4-dihydroquinoline-2-carboxylate (4.20 g, 0.017 mol) was dissolved in dry DMF (42 mL) under N_2. Then $POBr_3$ (6.45 g, 0.022 mol) was added. The reaction mixture was stirred for 5 h at 80 °C. After TLC confirmed the reaction completion, the mixture was poured into ice and neutralised with saturated $NaHCO_3$ solution. Then the mixture was extracted with DCM. The combined organic layers were washed with water and brine,

dried (Na_2SO_4) and then concentrated under reduced pressure to give 4.8 g (92%) of **10** as a solid.

^{1}H NMR (500 MHz, DMSO-d_6) δ 8.98 (d, J = 2.2 Hz, 1H), 8.59 (s, 1H), 8.58 (dd, J = 9.1, 2.2 Hz, 1H), 8.47 (d, J = 9.1 Hz, 1H), 4.00 (s, 3H).

^{13}C NMR (126 MHz, DMSO-d_6) δ 163.6, 149.8, 149.1, 146.3, 134.7, 131.1, 129.0, 127.3, 126.1, 123.5, 53.2.

HRMS: calcd. for $C_{11}H_7N_2O_4Br$ $[M]^-$ 309.9584; found 309.9594.

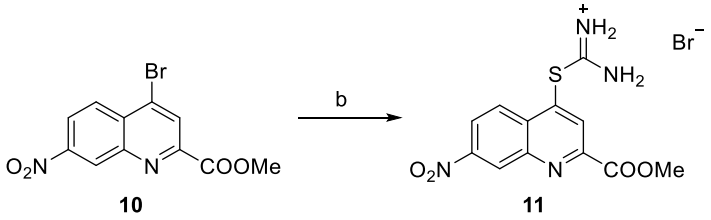

Compound 11. Compound **10** (4.76 g, 0.015 mol) and thiourea (2.33 g, 0.031 mol) were dissolved in acetone (75 mL). The reaction mixture was refluxed under N_2 for 3 h. After TLC confirmed the reaction completion, the reaction mixture was left to cool down to r.t.. The precipitate was filtered and washed with acetone and then dried under reduced pressure to give 5.47 g (93%) of **11** as a white powder.

^{1}H NMR (500 MHz, DMSO-d_6) δ 9.26 (s, 2H), 9.14 (s, 2H), 9.08 (d, J = 2.3 Hz, 1H), 8.67 (s, 1H), 8.63 (dd, J = 9.2, 2.3 Hz, 1H), 8.51 (d, J = 9.2 Hz, 1H), 4.03 (s, 3H).

^{13}C NMR (126 MHz, DMSO-d_6) δ 167.0, 164.0, 149.9, 149.0, 146.8, 134.9, 132.6, 132.3, 127.1, 126.3, 123.7, 53.3.

HRMS: calcd. for $C_{12}H_{11}N_4O_4S$ $[M+H]^+$ 307.0496; found 307.0496.

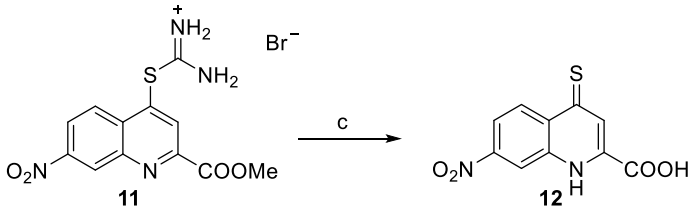

Compound 12. Compound **11** (5.47 g, 0.014 mol) was dissolved in MeOH (55 mL), then NaOH (2.83 g, 0.071 mol) in H_2O (17.6 mL) was added slowly. The mixture was stirred for 3 h at r.t.. After NMR confirmed the reaction completion, 1 M HCl was then added to acidify the mixture to approximately pH 4 to allow for full precipitation. The precipitate was filtered and washed with a small amount of water and then dried under reduced pressure to give 3.5 g (99%) of **12** as a dark red solid.

^{1}H NMR (500 MHz, DMSO-d_6) δ 9.00 (d, J = 2.3 Hz, 1H), 8.75 (d, J = 9.2 Hz, 1H), 8.19 (dd, J = 9.2, 2.4 Hz, 1H), 7.81 (s, 1H).

^{13}C NMR (126 MHz, DMSO-d_6) δ 195.2, 163.1, 149.7, 136.0, 135.5, 133.3, 130.3, 126.2, 119.3, 117.4.

HRMS: calcd. for $C_{10}H_5N_2O_4S$ $[M-H]^-$ 248.9965; found 248.9978.

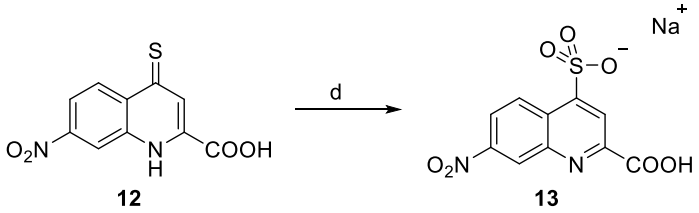

12 13

Compound 13. A solution of 30% H_2O_2 (4 mL, 0.04 mol) in formic acid (29 mL) was stirred at room temperature under N_2 for 1 h. Then a suspension of compound **12** (2.00 g, 0.008 mol) in formic acid (18 mL) was added carefully. The reaction mixture was stirred for 5 h at 48 °C under N_2. After HPLC confirmed the reaction completion, the reaction mixture was cooled to 0 °C by ice-bath and then NaCl solid was added slowly until a white precipitate formed. The precipitate was filtered while it was still cold. The solid was washed with a small amount of cold water and then dried under reduced pressure to give 1.00 g (40%) of **13** as a white powder.

^{1}H NMR (500 MHz, DMSO-d_6) δ 9.06 (d, J = 9.3 Hz, 1H), 8.67 (s, 1H), 8.92 (d, J = 2.4 Hz, 1H), 8.49 (dd, J = 9.3, 2.4 Hz, 1H).

^{13}C NMR (126 MHz, DMSO-d_6) δ 165.5, 153.5, 151.0, 148.0, 146.7, 129.7, 128.0, 125.4, 121.4, 120.1.

HRMS: calcd. for $C_{10}H_5N_2O_7S$ $[M-H]^-$ 296.9812; found 296.9824.

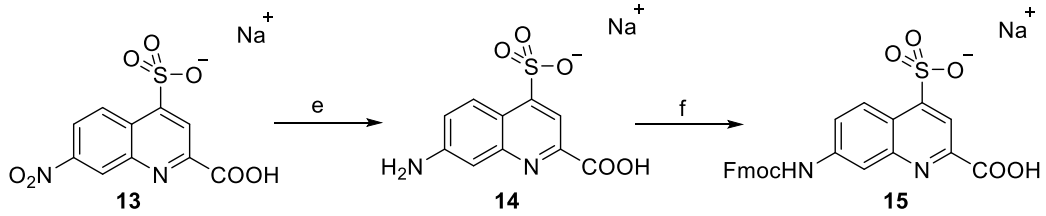

13 14 15

Compound 15. Compound **13** (0.96 g, 0.003 mol) was dissolved in MeOH (221 mL) under N_2. Then 10 wt.% Pd/C (0.34 g, 35% *w*/*w*) was added and N_2 was replaced by H_2. The mixture was stirred for 4 h at r.t. and then another 10 wt.% Pd/C (0.34 g, 35% *w*/*w*) was added and the mixture was stirred for another 4 h. The resulting mixture was filtered through celite and solvents were evaporated under reduced pressure to give **14** as a bright yellow powder which was used directly in the next step without further purification. **14** was dissolved in 10% (*w*/*w*) $NaHCO_3$ solution (58 mL) and the mixture was cooled down to 0 °C. Fmoc-Cl (1086 mg, 0.004

mol) in dioxane (34 mL) was added dropwise at 0 °C to the resulting slurry over 1 h. The mixture was stirred at 0 °C for another hour, and allowed to warm to room temperature overnight. After TLC confirmed the reaction completion, the solution was acidified to pH = 4 using 1 M HCl solution. The aqueous mixture was washed several times with Et_2O until precipitation formed. The solid was filtered and washed with Et_2O and a small amount of H_2O. The resulting solid was dried under reduced pressure to give 860 mg (56%) of **15** as a yellow powder. Note: Additional experiments indicated the product contains some sodium salt; nevertheless, the salt doesn't affect the use of SPS.

^{1}H NMR (500 MHz, DMSO-d_6) δ 10.21 (s, 1H), 8.73 (d, J = 9.3 Hz, 1H), 8.34 (s, 1H), 8.23 (s, 1H), 7.93 (dt, J = 7.6, 1.0 Hz, 2H), 7.81 (dd, J = 7.5, 1.1 Hz, 2H), 7.77 (d, J = 9.4 Hz, 1H), 7.45 (td, J = 7.7, 1.1 Hz, 2H), 7.38 (td, J = 7.5, 1.2 Hz, 2H), 4.58 (d, J = 6.6 Hz, 2H), 4.37 (t, J = 6.6 Hz, 1H).

^{13}C NMR (126 MHz, DMSO-d_6) δ 166.5, 153.9, 153.5, 148.9, 148.9, 144.2, 141.3, 141.0, 128.3, 128.2, 127.6, 125.7, 121.9, 121.1, 120.7, 116.7, 115.2, 66.4, 47.1.

HRMS: calcd. for $C_{25}H_{17}N_2O_7S$ $[M-H]^-$ 489.0751; found 489.0763.

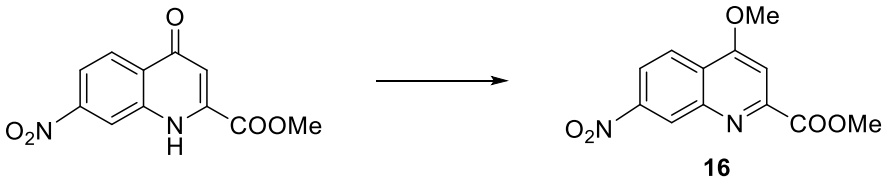

16

Compound 16. Methyl 7-nitro-4-oxo-1,4-dihydroquinoline-2-carboxylate (1 g, 0.040 mmol), PPh3 (1.59 g, 0.061 mmol) and MeOH (245 μL, 0.060 mmol) were dissolved in THF (30 mL) under N_2. Then diisopropyl azodicarboxylate (1.2 mL, 0.060 mmol) was added dropwise. The mixture was stirred for 14 h at r.t.. After TLC confirmed the reaction completion, the mixture was filtered and concentrated. The residue was precipitated in MeOH to give 600 mg (57%) of **16** as a white solid.

^{1}H NMR (500 MHz, DMSO-d_6) δ 8.86 (d, J = 2.1 Hz, 1H), 8.43 (d, J = 9.2 Hz, 1H), 8.39 (dd, J = 9.2, 2.2 Hz, 1H), 7.72 (s, 1H), 4.20 (s, 3H), 3.99 (s, 3H).

^{13}C NMR (126 MHz, DMSO-d_6) δ 164.9, 162.9, 151.4, 148.7, 146.8, 125.1, 124.7, 124.1, 120.9, 102.9, 57.0, 53.0.

HRMS: calcd. for $C_{12}H_{11}N_2O_5$ $[M+H]^+$ 263.0662; found 263.0769.

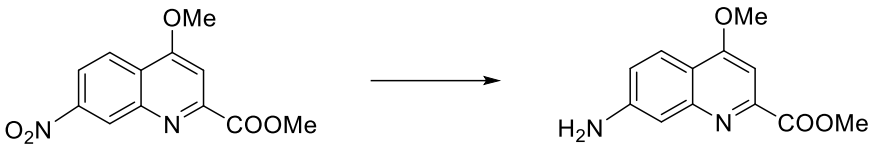

Compound 17. Compound **16** (3.97 g, 0.015 mmol) was dissolved in THF (266 mL) and MeOH (400 mL) under N_2. Then 10 wt.% Pd/C (1 g, 35% *w*/*w*) was added and N_2 was replaced by H_2. The mixture was stirred for 3 h at room temperature. After TLC confirmed the reaction completion, the mixture was filtered and concentrated to give 3.49 g (99%) of **17** as a yellow powder.

^{1}H NMR (500 MHz, DMSO-d_6) δ 7.85 (d, *J* = 8.9 Hz, 1H), 7.20 (s, 1H), 7.03 (dd, *J* = 8.9, 2.2 Hz, 1H), 6.95 (d, *J* = 2.2 Hz, 1H), 5.89 (s, 2H), 4.02 (s, 3H), 3.90 (s, 3H).

^{13}C NMR (126 MHz, DMSO-d_6) δ 166.0, 162.4, 151.1, 150.4, 148.7, 122.1, 119.6, 112.9, 106.8, 96.8, 55.9, 52.4.

HRMS: calcd. for $C_{12}H_{12}N_2O_3Na$ $[M+Na]^+$ 255.0740; found 255.0739.

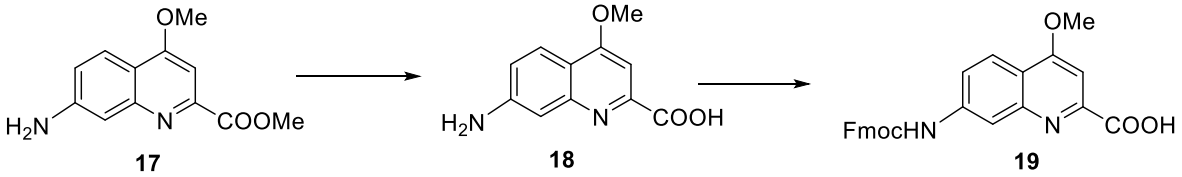

Compound 19. Compound **17** (3.81 g, 0.016 mol) was dissolved in dioxane (324 mL) then $LiOH{\cdot}H_2O$ (1.03 g, 0.024 mol) in water (102 mL) was added slowly at 0 °C. The mixture was stirred for 1 h at 0 °C, then neutralized by 0.1 mol·L^{-1} HCl. Then water (120 mL) and $NaHCO_3$ (4.13 g, 0.049 mol) were added and cooled down to 0 °C by ice-bath. Fmoc-Cl (5.52 g, 0.02 mol) is added slowly as a solution in dioxane. The resulting mixture is stirred at 0 °C for 1 h and allowed to warm to room temperature overnight. After TLC confirmed the reaction completion, the solution was acidified to pH = 4 using a saturated citric acid solution. Then water was added and the aqueous layers were extracted with DCM. The combined organic layers were washed with water and brine, dried (Na_2SO_4) and then concentrated under reduced pressure. The residue was triturated and sonicated in DCM, acetonitrile and water. The final slurry was lyophilized to give 5.06 g (70%) of **19** as a yellow powder.

^{1}H NMR (500 MHz, DMSO-d_6) δ 10.23 (s, 1H), 8.30 (s, 1H), 8.09 (d, *J* = 9.0 Hz, 1H), 7.92 (d, *J* = 7.5 Hz, 2H), 7.78 (d, *J* = 7.4 Hz, 2H), 7.73 (d, *J* = 8.2 Hz, 1H), 7.45 (s, 1H), 7.43 (t, *J* = 7.5 Hz, 2H), 7.36 (td, *J* = 7.4, 1.2 Hz, 2H), 4.59 (d, *J* = 6.5 Hz, 2H), 4.36 (t, *J* = 6.5 Hz, 1H), 4.10 (s, 3H).

^{13}C NMR (126 MHz, DMSO-d_6) δ 165.9, 163.1, 153.4, 150.9, 147.8, 143.7, 141.4, 140.8, 127.7, 127.2, 125.1, 122.3, 120.4, 120.2, 116.8, 114.2, 99.1, 65.8, 56.4, 46.6.

HRMS: calcd. for $C_{26}H_{21}N_2O_5$ $[M+H]^+$ 441.1445; found 441.1447.

3 **X-ray crystallographic analysis of the structure of (5)$_2$**

Aqueous solution of (**5**)$_2$ was prepared by dissolving the lyophilized powder in water to a final concentration of 5mM. Crystallization trials were carried with commercial sparse matrix screens using standard sitting drop vapor diffusion method at 293 K. X-ray quality crystals were obtained after three weeks by the addition of 0.8 µl of (**1**)$_2$ and 0.8 µl of 15% w/v polyethylene glycol 8000, 100 mM MES buffer at pH 6.5 and 200 mM calcium acetate in the reservoir. For low temperature diffraction measurement, a crystal was fished using a microloop, cryo-protected using 30% v/v polyethylene glycol 400 and plunged into liquid nitrogen.

X-ray diffraction data was collected at the ID30B[7] beamline in European Synchrotron Radiation Facility (ESRF), Grenoble. Diffraction data was measured at T = 100 K, λ = 0.9184 Å. The crystal was exposed for 0.02 s and 0.2° oscillation per frame and a rotation pass of 360° was measured using a EIGER2 X 9M 450µm Si sensor (Dectris) detector. Diffraction data was processed using the program *XDS*[8]. The crystal belonged to the space group *P*-1 with unit cell parameters: a = 25.288 (3) Å, b = 27.896 (4) Å, c = 41.288 (2) Å, α = 90.710 (4)°, β = 99.819 (1)°, γ = 116.180 (1)°; V = 25629 (6) Å^3 and two helices per asymmetric unit (Z = 4, Z' = 2). The structure was solved with *SHELXT*[9] structure solution program using Intrinsic Phasing and refined by full-matrix least-squares method on F^2 with *SHELXL*-2014[10] within *Olex2*[11]. After each refinement step, visual inspection of the model and the electron-density maps were carried out using *Olex2*[11] and *Coot*[12] using $2F_o - F_c$ and difference Fourier ($F_o - F_c$) maps. The initial structure revealed all main-chain atoms of a double-helical capsule. The CH_3 group of diethylene glycol tail was severely disordered in both helices and omitted. AFIX, SADI, DFIX and FLAT instructions were used to improve the geometry of molecules. Restraints on anisotropic displacement parameters were implemented with DELU, ISOR and EADP instructions. All non-H atoms were refined with anisotropic displacement parameters. After several attempts to model the disordered side chains and diethylene glycol tail, the SQUEEZE[13] procedure was used to flatten the electron density map. Very disordered solvent molecules were removed. Calculated total potential solvent accessible void volume and electron count per cell are 7403.1 Å^3 and 2220 respectively. Hydrogen atoms for (**5**)$_2$ were placed at idealized positions.

Statistics of data collection and refinement of (**5**)$_2$ are described in Table S1. The final cif file of (**5**)$_2$ was examined in IUCr's *checkCIF* algorithm. Due to the large volume fractions of disordered solvent molecules, weak diffraction intensity and poor resolution, a number of A- and B- level alerts remain in the *checkCIF* file. These alerts are inherent to the data set and

refinement procedures. They are listed below and were divided into two groups. The first group demonstrates weak quality of the data and refinement statistics when compared to those expected for small molecule structures from highly diffracting crystals. The second group is concerned to decisions made during refinement and explained below. Atomic coordinates and structure factors of (**5**)$_2$ was deposited in the Cambridge Crystallographic Data Centre (CCDC) with accession code 2216788. The data is available free of charge upon request (www.ccdc.cam.ac.uk/).

CheckCIF validation of (**1**)$_2$:

Group 1 alerts (these illustrate weak quality of data and refinement statistics if compared to small molecule structures from highly diffracting crystals):

THETM01_ALERT_3_A The value of sine(theta_max)/wavelength is less than 0.550
Calculated sin(theta_max)/wavelength = 0.4762
PLAT029_ALERT_3_A _diffrn_measured_fraction_theta_full value Low . 0.917
PLAT084_ALERT_3_B High wR2 Value (i.e. > 0.25) ..... 0.44 Report
PLAT241_ALERT_2_B High 'MainMol' Ueq as Compared to Neighbors of Check
PLAT242_ALERT_2_B Low 'MainMol' Ueq as Compared to Neighbors of Check
PLAT260_ALERT_2_B Large Average Ueq of Residue Including O0F5 0.353 Check
PLAT260_ALERT_2_B Large Average Ueq of Residue Including O0F9 0.310 Check
PLAT340_ALERT_3_B Low Bond Precision on C-C Bonds 0.01725 Ang.
PLAT414_ALERT_2_B Short Intra XH3 .. XHn H30C ..H302 1.75 Ang.
PLAT430_ALERT_2_A Short Inter D...A Contact O016 ..O277 2.76 Ang.

Group 2 alert (is connected with decision made during refinement and explained below):

PLAT196_ALERT_1_B No TEMP record and _measurement_temperature .NE. 293 Degree
Measurement temperature was 100 K.
PLAT306_ALERT_2_B Isolated Oxygen Atom (H-atoms Missing ?) Check
Dummy O atom was introduced into refinement.
PLAT780_ALERT_1_B Coordinates do not Form a Properly Connected Set
The connected set is through individual helices in the double helical capsule.

Table S1. Crystallographic data and refinement details for $(\mathbf{5})_2$.

Identification code	$(\mathbf{1})_2$
Emperical formula	$C_{159}\,H_{108.5}\,Ca\,N_{29}\,O_{62.5}\,S_6$
Formula weight	3657.68
Temperature	100 K
Wavelength	0.9184 Å
Crystal system	Triclinic
Space group	*P*-1
Unit cell dimensions	a = 25.288 (3) Å b = 27.896 (4) Å c = 41.288 (2) Å α = 90.710 (4)° β = 99.819 (1)° γ = 116.180 (1)°
Volume	25629 (5) $Å^3$
Z	4
Density (calculated)	0.948 g/cm^3
Absorption coefficient	0.266 μ/mm^{-1}
Colour and shape	Pale yellow, prism
Crystal size	0.200 x 0.100 x 0.050 mm
Index ranges	$-23 \leq h \leq 23$ $-26 \leq k \leq 26$ $-39 \leq l \leq 39$
Reflections collected	137893
R_{int}	0.0663
Data/restraints/parameters	42538/223/4438
Goodness-of-fit on F^2	1.909
Final R indexes [$I > 2\sigma(I)$]	R_1 = 0.1361 wR_2 = 0.4112
Final R indexes [all data]	R_1 = 0.1527 wR_2 = 0.4398
Largest diff. peak and hole	1.16/-0.65 e $Å^{-3}$
CCDC #	2216788

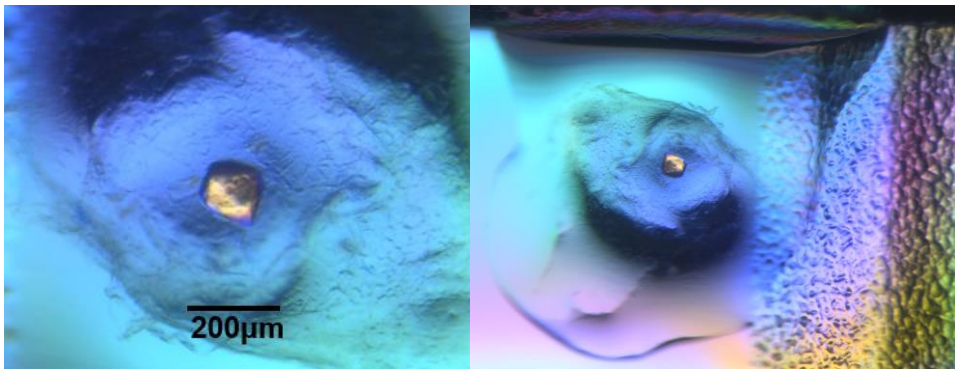

Figure S24.: Single crystal of $(\mathbf{5})_2$ observed under cross-polarizing microscope

4 NMR spectra and RP-HPLC chromatograms of new compounds

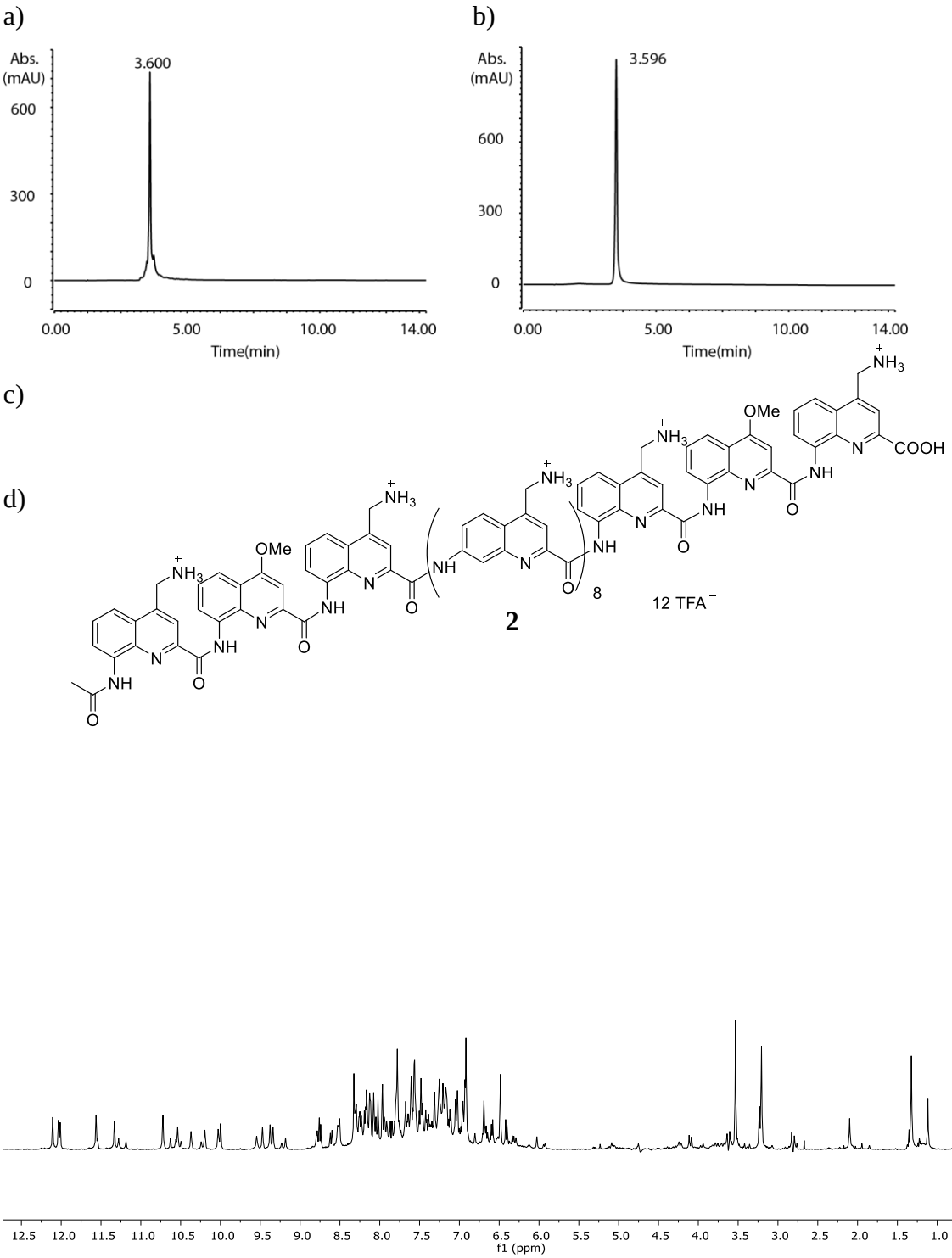

Figure S25. Analytical data of compound **2**. RP-HPLC chromatograms (a) recovered crude from TFA cleavage (C18, 5 to 100 B% over 10 min, λ = 300 nm) and (b) after purification (C18, 5 to 100 B% over 10 min, λ = 300 nm); A: 0.1% TFA water, B: 0.1% TFA acetonitrile. (c) Chemical structure of compound **2**. (d) ^{1}H NMR spectrum with water suppression (500 MHz, H_2O/D_2O = (9:1, *v*/*v*), 25 °C).

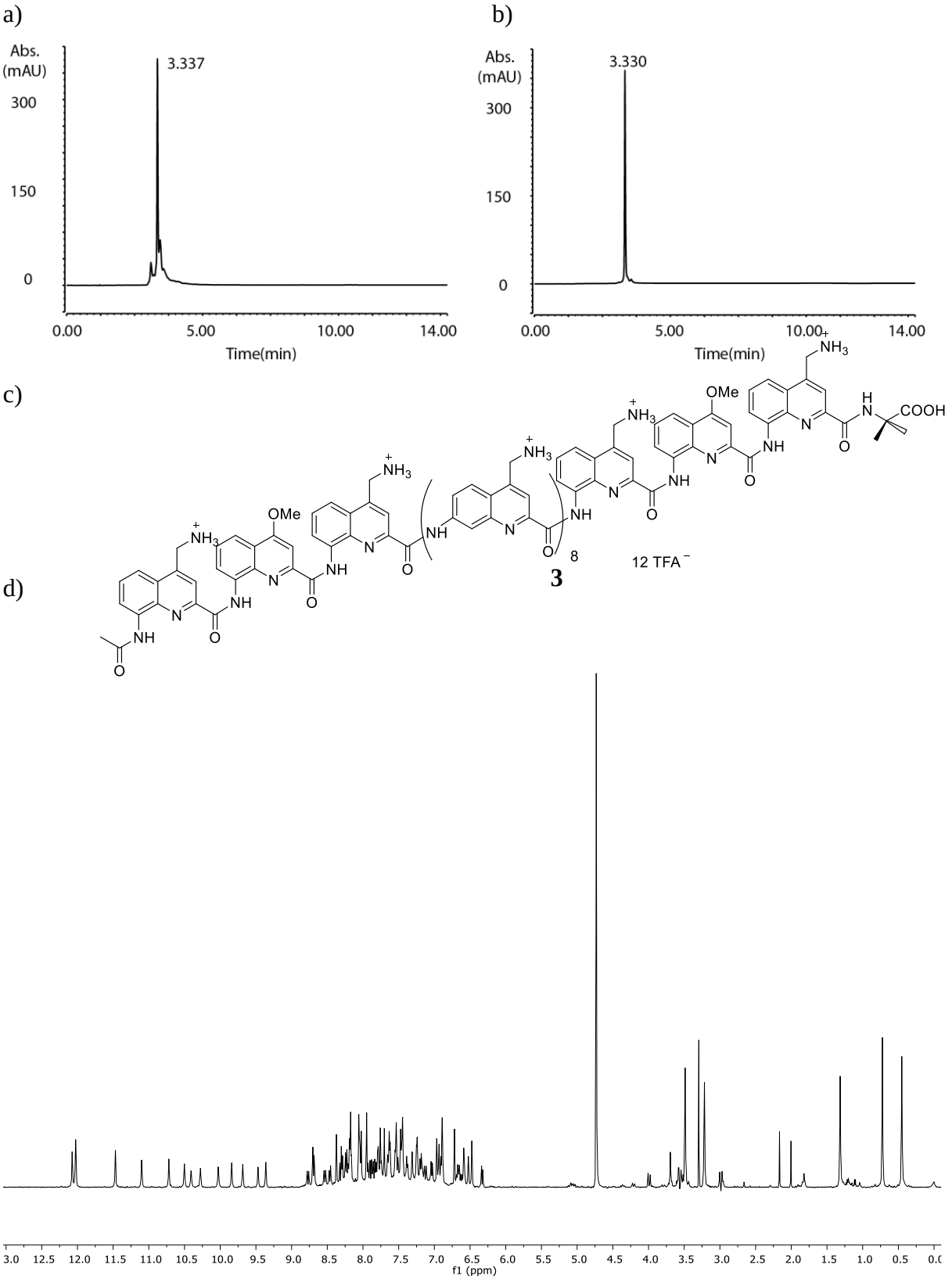

Figure S26. Analytical data of compound **3**. RP-HPLC chromatograms (a) recovered crude from TFA cleavage (C18, 5 to 100 B% over 10 min, λ = 300 nm) and (b) after purification (C18, 5 to 100 B% over 10 min, λ = 300 nm); A: 0.1% TFA water, B: 0.1% TFA acetonitrile. (c) Chemical structure of compound **3**. (d) ^{1}H NMR spectrum with water suppression (500 MHz, H_2O/D_2O (9:1, *v*/*v*), 25 °C).

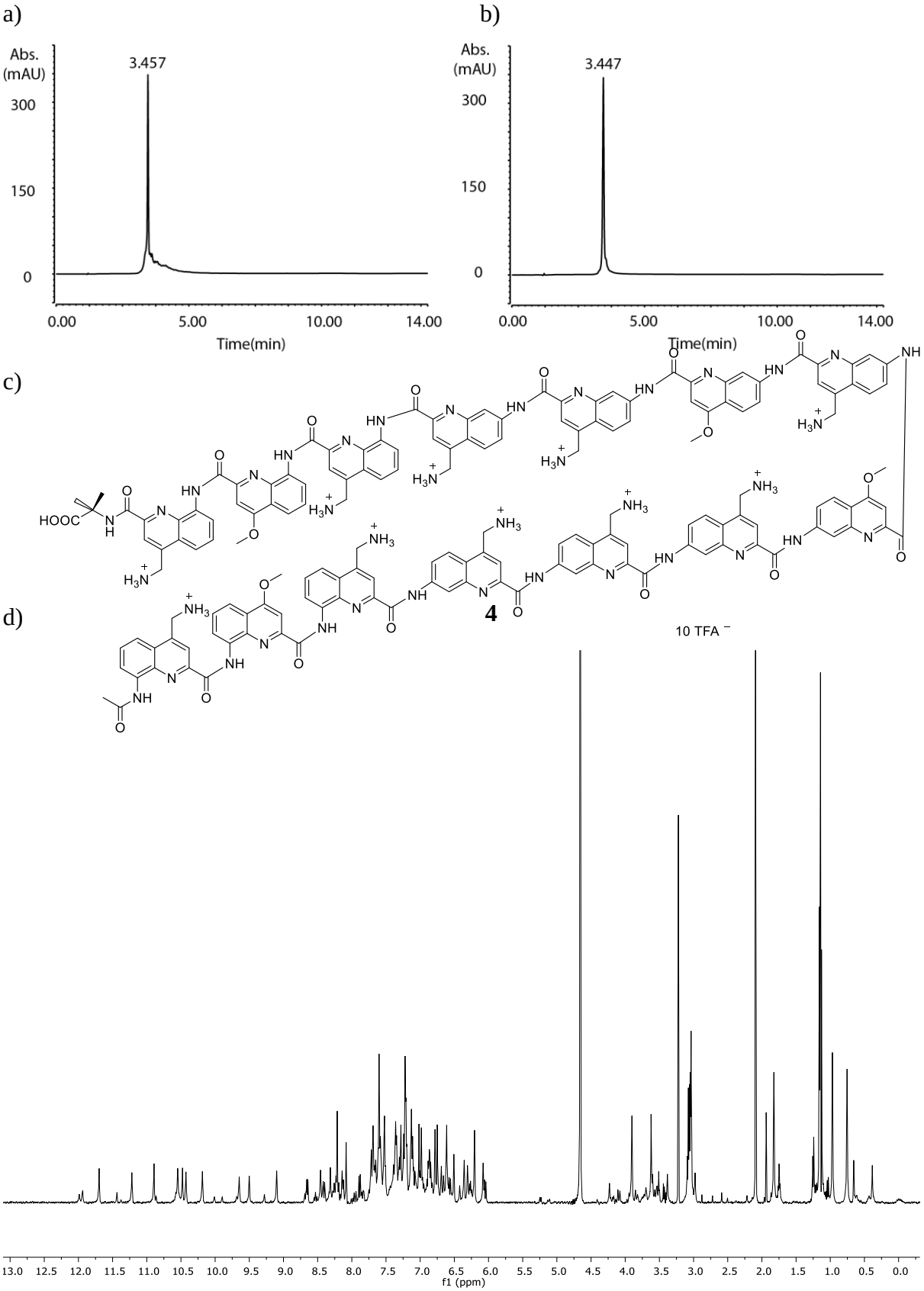

Figure S27. Analytical data of compound **4**. RP-HPLC chromatograms (a) recovered crude from TFA cleavage (C18, 5 to 100 B% over 10 min, λ = 300 nm) and (b) after purification (C18, 5 to 100 B% over 10 min, λ = 300 nm); A: 0.1% TFA water, B: 0.1% TFA acetonitrile. (c) Chemical structure of compound **4**. (d) ^{1}H NMR spectrum with water suppression (500 MHz, H_2O/D_2O (9:1, *v*/*v*), 25 °C).

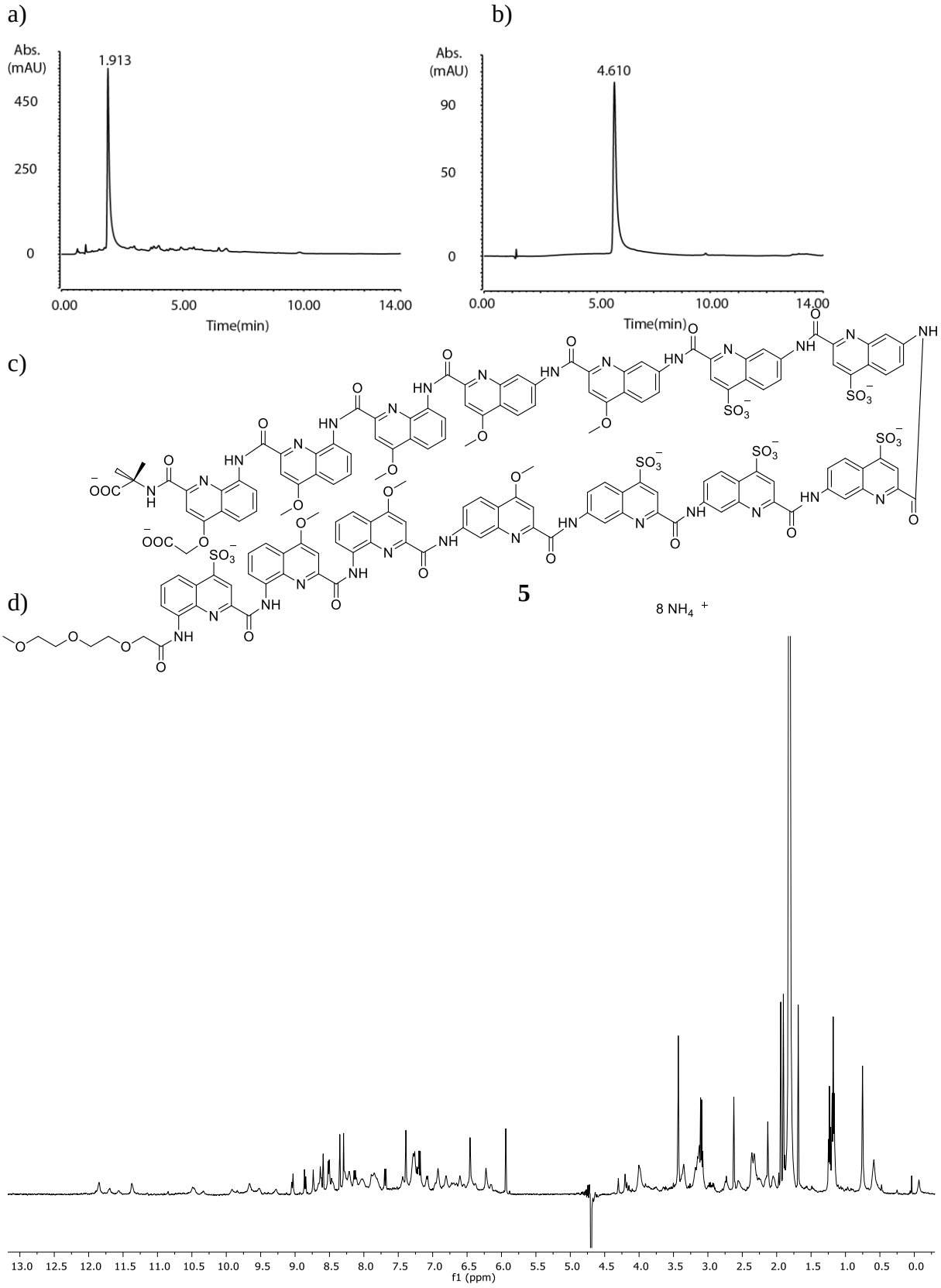

Figure S28. Analytical data of compound **5**. RP-HPLC chromatograms (a) recovered crude from TFA cleavage (C18, 30 to 80 B% over 10 min, λ = 300 nm) and (b) after purification (C18, 10 to 40 B% over 10 min, λ = 300 nm; A: 13 mM ammonium acetate aqueous buffer pH 8.5, B: acetonitrile). (c) Chemical structure of compound **5**. (d) ^{1}H NMR spectrum with water suppression (500 MHz, ammonium acetate aqueous buffer pH 8.5/D_2O (9:1, *v*/*v*), 25 °C).

a)

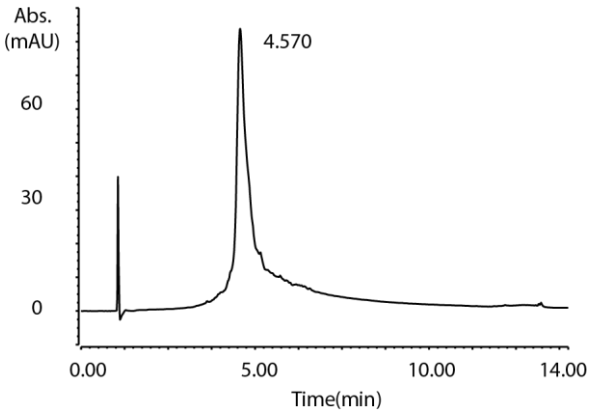

b)

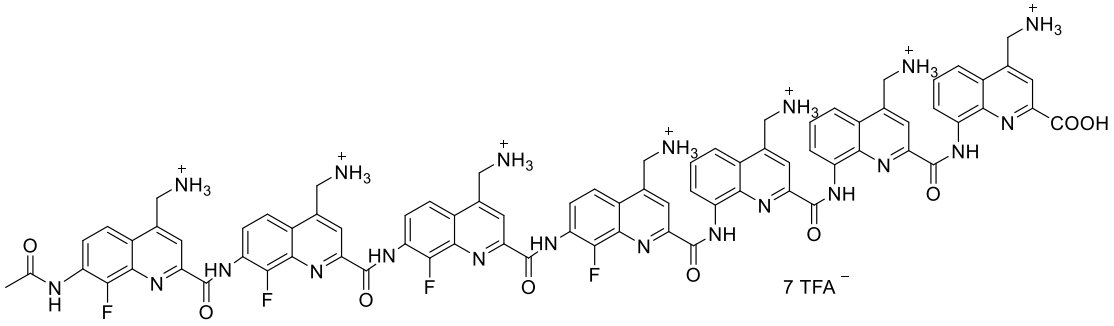

c) **6**

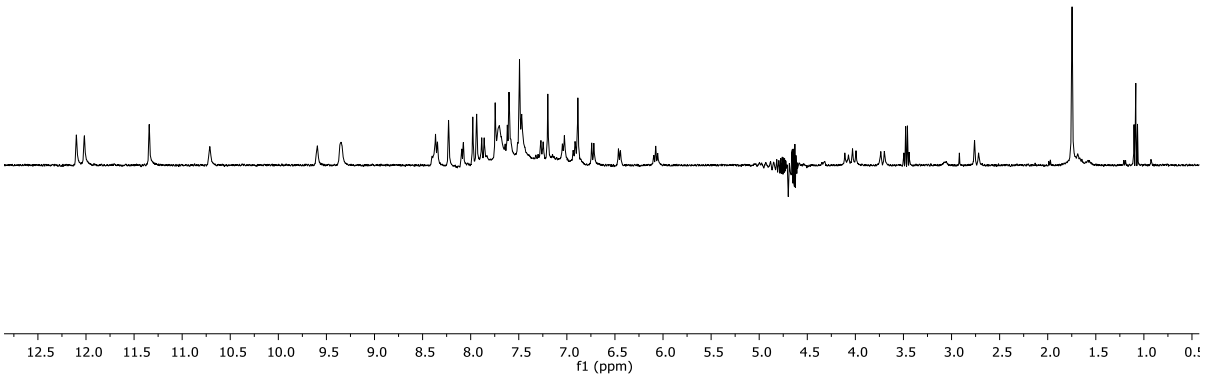

Figure S29. Analytical data of compound **6**. RP-HPLC chromatograms (a) recovered crude from TFA cleavage (C18, 5 to 60 B% over 10 min, λ = 300 nm); A: 0.1% TFA water, B: 0.1% TFA acetonitrile. (b) Chemical structure of compound **6**. (c) ^{1}H NMR spectrum with water suppression (400 MHz, H_2O/D_2O (9:1, *v*/*v*), 25 °C).

a)

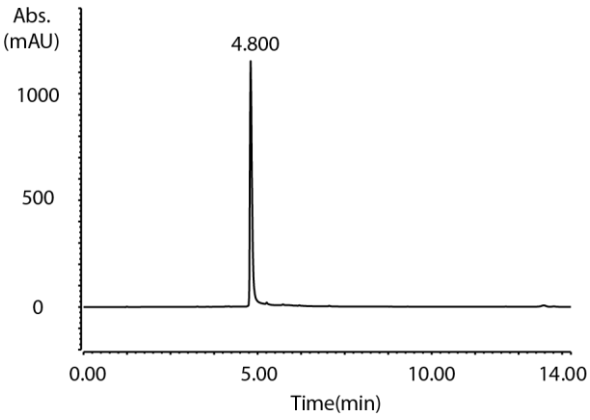

b)

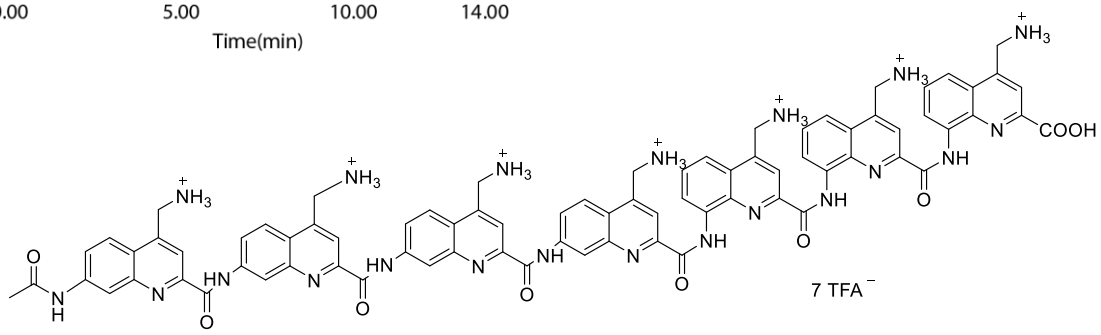

7

c)

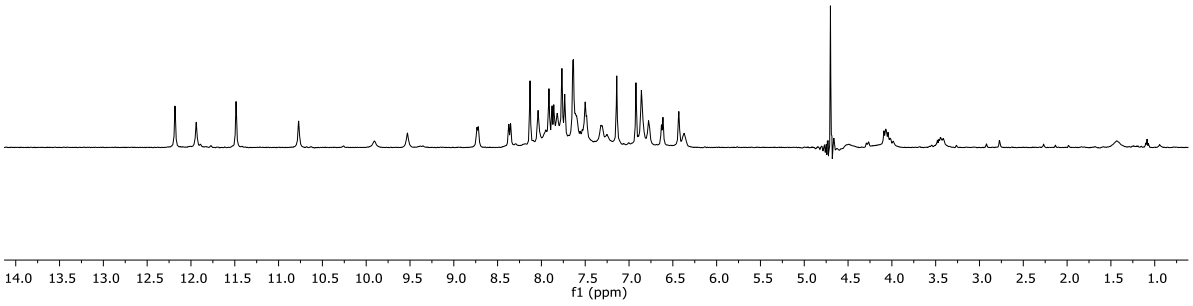

Figure S30. Analytical data of compound **7**. RP-HPLC chromatograms (a) recovered crude from TFA cleavage (C18, 5 to 60 B% over 10 min, λ = 300 nm); A: 0.1% TFA water, B: 0.1% TFA acetonitrile. (b) Chemical structure of compound **7**. (c) ^{1}H NMR spectrum with water suppression (500 MHz, H_2O/D_2O (9:1, *v*/*v*), 25 °C).

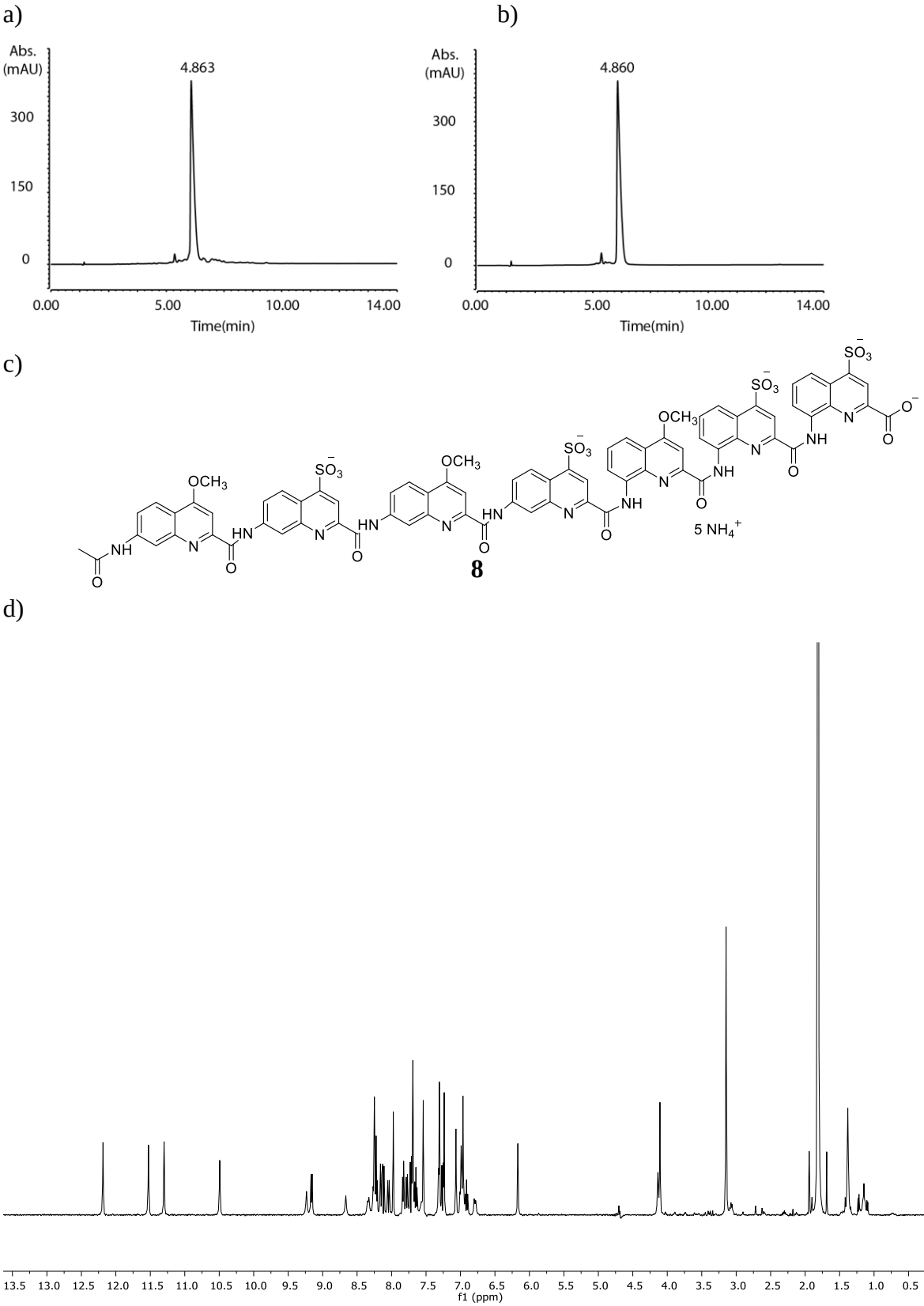

Figure S31. Analytical data of compound **8**. RP-HPLC chromatograms (a) recovered crude from TFA cleavage (C18, 10 to 80 B% over 10 min, λ = 300 nm) and (b) after purification (C18, 10 to 80B% over 10 min, λ = 300 nm; A: 13 mM ammonium acetate aqueous buffer pH 8.5, B: acetonitrile). (c) Chemical structure of compound **8**. (d) ^{1}H NMR spectrum with water suppression (500 MHz, ammonium acetate aqueous buffer pH 8.5/D_2O (9:1, *v*/*v*), 25 °C).

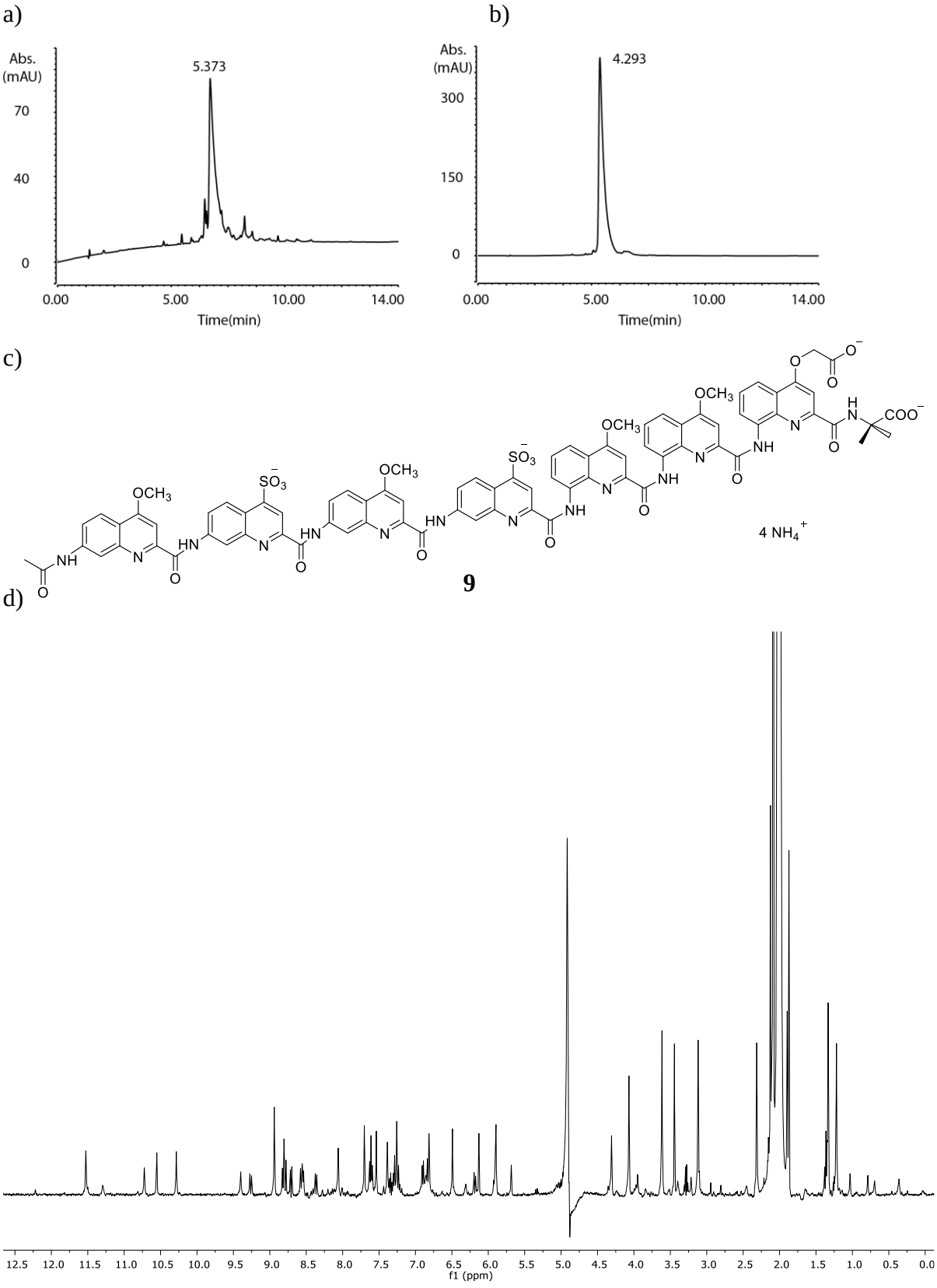

Figure S32. Analytical data of compound **9**. RP-HPLC chromatograms (a) recovered crude from TFA cleavage (C18, 10 to 60 B% over 10 min, λ = 300 nm) and (b) after purification (C18, 10 to 80B% over 10 min, λ = 300 nm; A: 13 mM ammonium acetate aqueous buffer pH 8.5, B: acetonitrile). (c) Chemical structure of compound **9**. (d) ^{1}H NMR spectrum with water suppression (500 MHz, ammonium acetate aqueous buffer pH 8.5/D_2O (9:1, *v*/*v*), 25 °C).

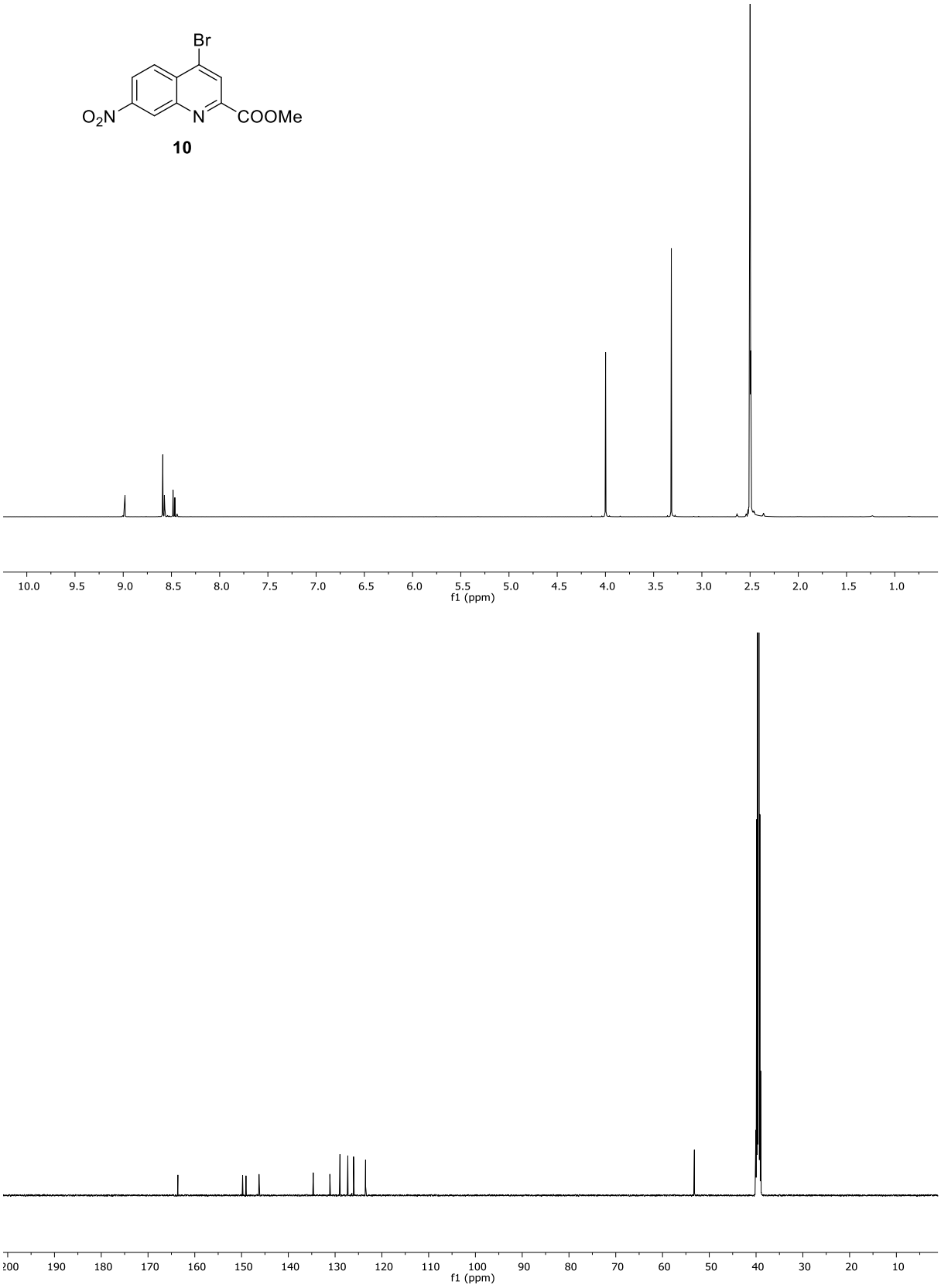

Figure S33. NMR spectra of compound **10** : ^{1}H NMR (500 MHz, DMSO-d_6) and ^{13}C NMR (126 MHz, DMSO-d_6).

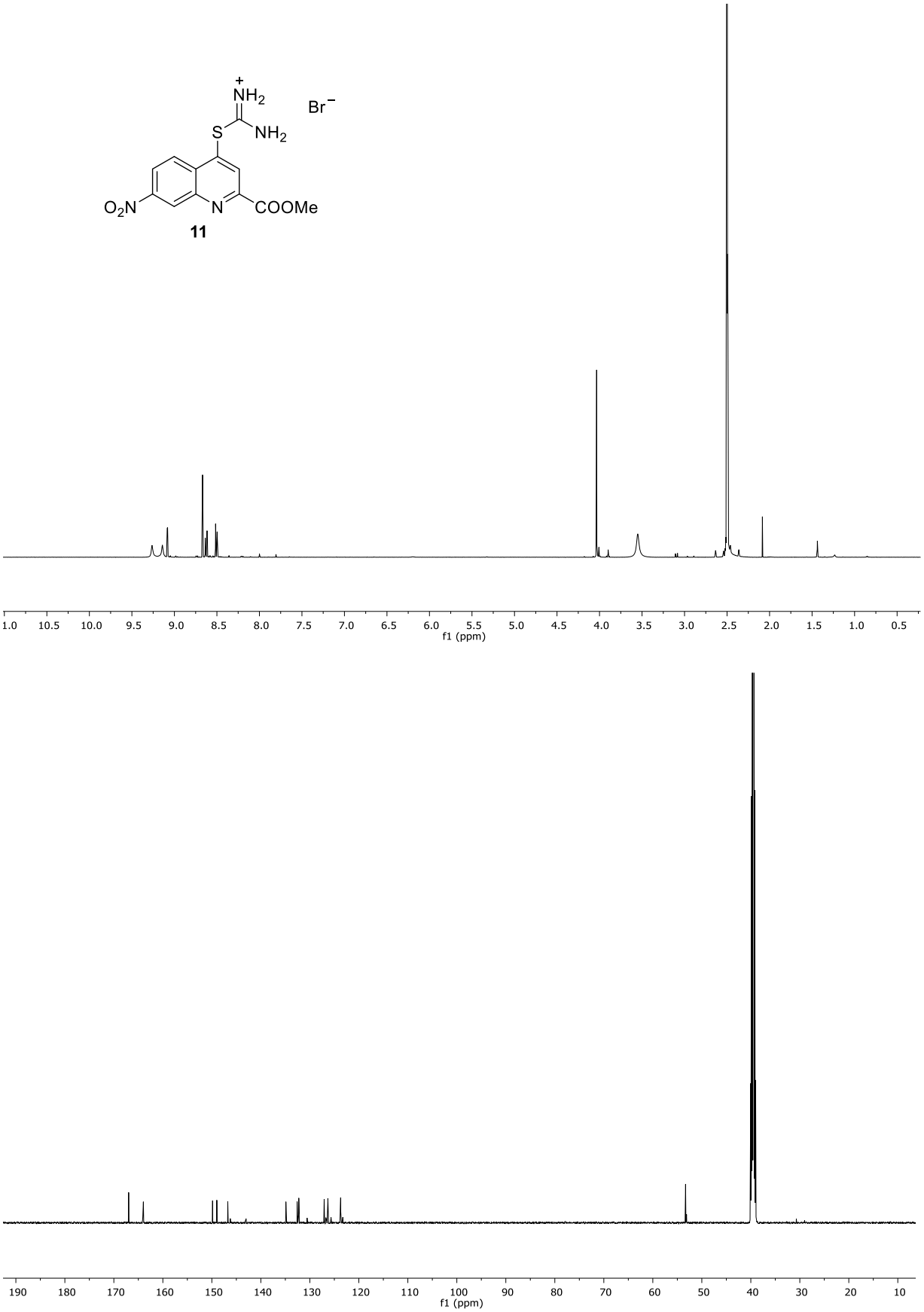

Figure S34. NMR spectra of compound **11** : ^{1}H NMR (500 MHz, DMSO-d_6) and ^{13}C NMR (126 MHz, DMSO-d_6).

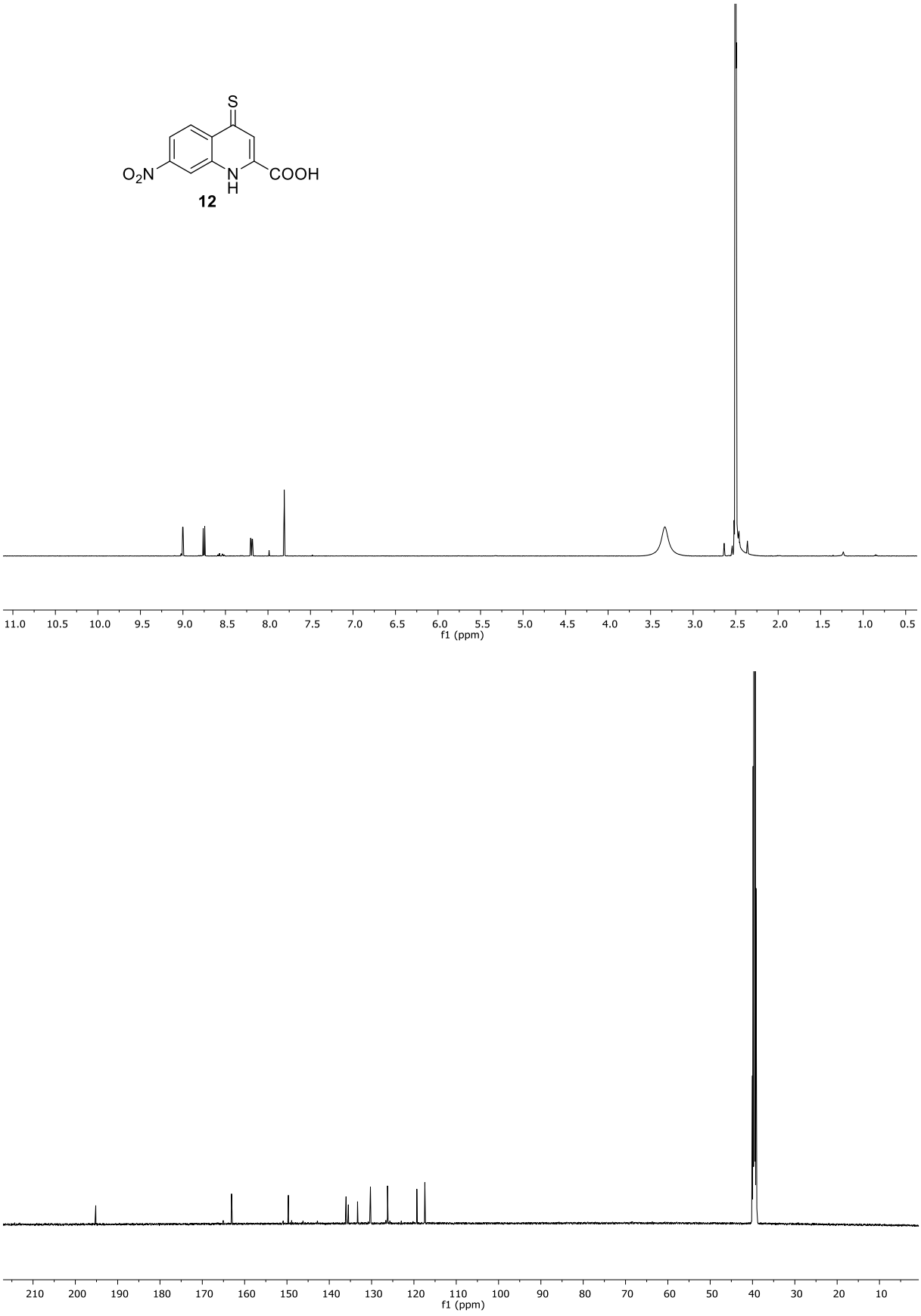

Figure S35. NMR spectra of compound **12** : ^{1}H NMR (500 MHz, DMSO-d_6) and ^{13}C NMR (126 MHz, DMSO-d_6).

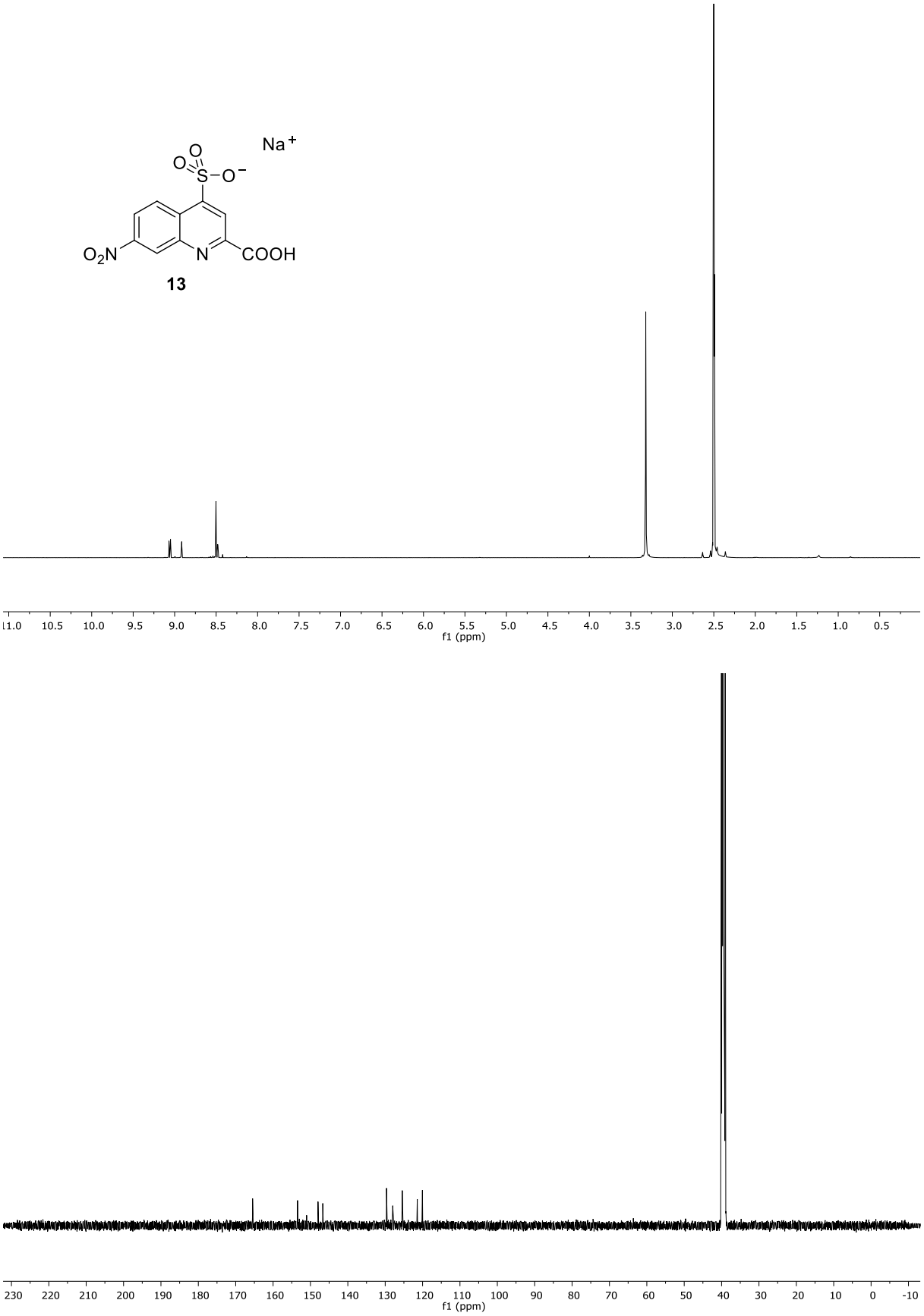

Figure S36. NMR spectra of compound **13** : ^{1}H NMR (500 MHz, DMSO-d_6) and ^{13}C NMR (126 MHz, DMSO-d_6).

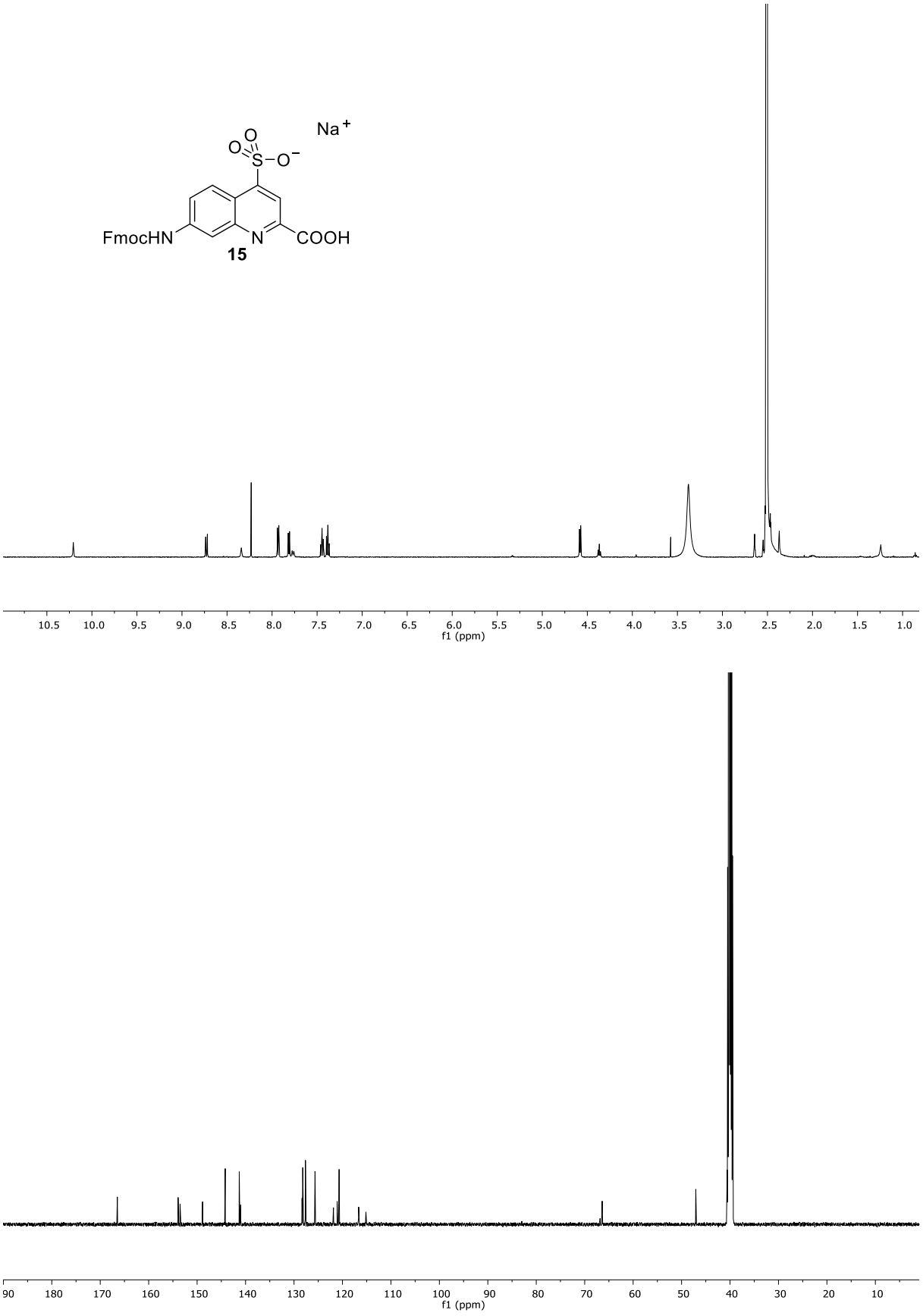

Figure S37. NMR spectra of compound **15** : ^{1}H NMR (500 MHz, DMSO-d_6) and ^{13}C NMR (126 MHz, DMSO-d_6).

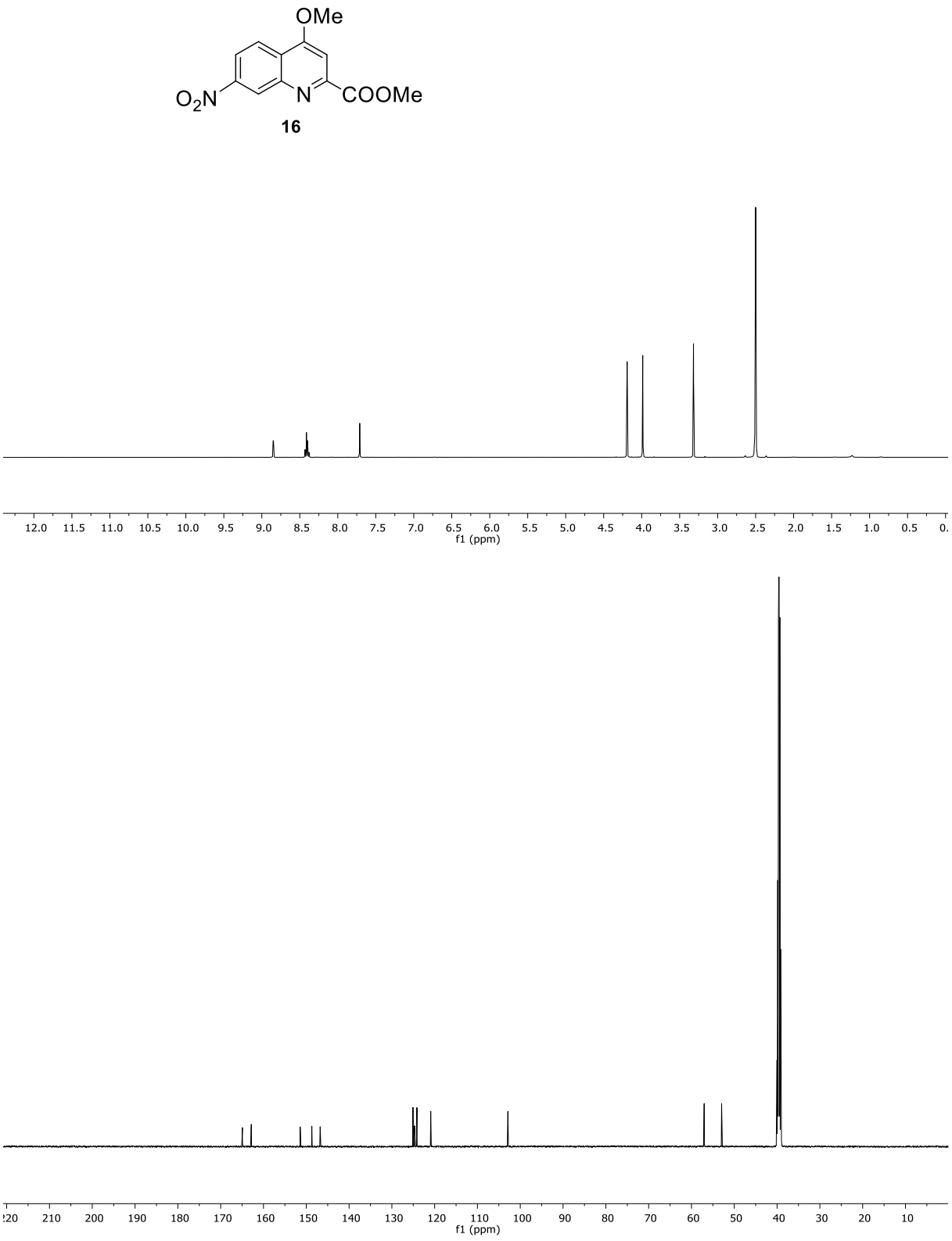

Figure S38. NMR spectra of compound **16** : ^{1}H NMR (500 MHz, DMSO-d_6) and ^{13}C NMR (126 MHz, DMSO-d_6).

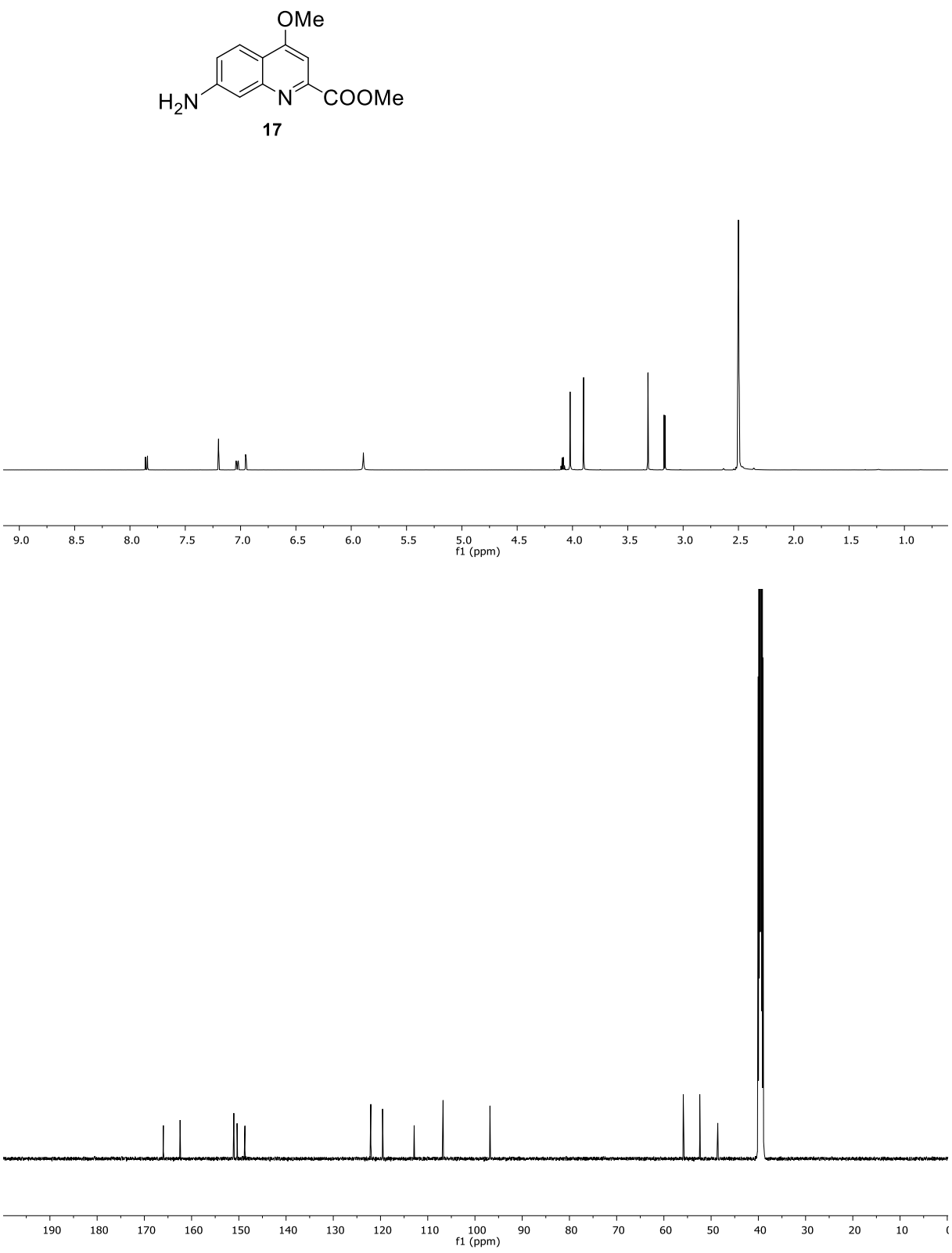

Figure S39. NMR spectra of compound **17** : ^{1}H NMR (500 MHz, DMSO-d_6) and ^{13}C NMR (126 MHz, DMSO-d_6).

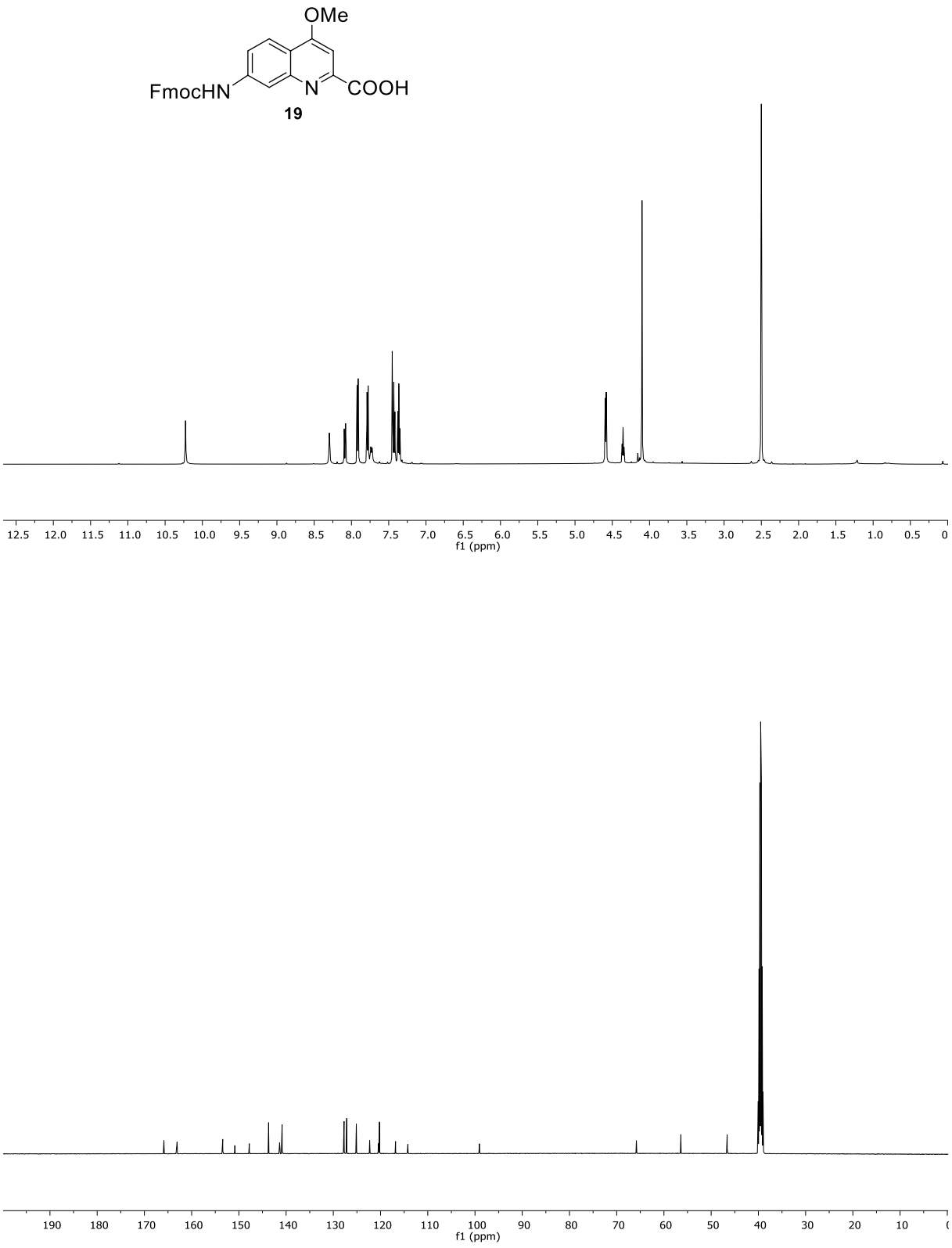

Figure S40. NMR spectra of compound **19** : ^{1}H NMR (500 MHz, DMSO-d_6) and ^{13}C NMR (126 MHz, DMSO-d_6).

5 Reference

1 B. Teng, J. Atcher, L. Allmendinger, C. Douat, Y. Ferrand and I. Huc, *Org. Biomol. Chem.*, 2023, DOI: 10.1039/D3OB00473B.

2 J. Buratto, C. Colombo, M. Stupfel, S. J. Dawson, C. Dolain, B. Langlois d'Estaintot, L. Fischer, T. Granier, M. Laguerre, B. Gallois and I. Huc, *Angew. Chem. Int. Ed.*, 2014, **53**, 883–887.

3 X. Hu, S. J. Dawson, P. K. Mandal, X. de Hatten, B. Baptiste and I. Huc, *Chem. Sci.*, 2017, **8**, 3741–3749.

4 B. Baptiste, C. Douat-Casassus, K. Laxmi-Reddy, F. Godde and I. Huc, *J. Org. Chem.*, 2010, **75**, 7175–7185.

5 S. Dengler, P. K. Mandal, L. Allmendinger, C. Douat and I. Huc, *Chem. Sci.*, 2021, **12**, 11004–11012.

6 V. Corvaglia, F. Sanchez, F. S. Menke, C. Douat, and I. Huc, *Chem. Eur. J*, 2023, DOI: 10.1002/chem.202301120.

7 A. A. McCarthy, R. Barrett, A. Beteva, H. Caserotto, F. Dobias, F. Felisaz, T. Giraud, M. Guijarro, R. Janocha, A. Khadrouche, M. Lentini, G. A. Leonard, M. Lopez Marrero, S. Malbet-Monaco, S. McSweeney, D. Nurizzo, G. Papp, C. Rossi, J. Sinoir, C. Sorez, J. Surr, O. Svensson, U. Zander, F. Cipriani, P. Theveneau and C. Mueller-Dieckmann, *J Synchrotron Rad*, 2018, **25**, 1249–1260.

8 W. Kabsch, *Acta Cryst D*, 2010, **66**, 125–132.

9 G. M. Sheldrick, *Acta Cryst A*, 2015, **71**, 3–8.

10 G. M. Sheldrick, *Acta Cryst C*, 2015, **71**, 3–8.

11 O. V. Dolomanov, L. J. Bourhis, R. J. Gildea, J. a. K. Howard and H. Puschmann, *J Appl Cryst*, 2009, **42**, 339–341.

12 P. Emsley, B. Lohkamp, W. G. Scott and K. Cowtan, *Acta Cryst D*, 2010, **66**, 486–501.

13 A. L. Spek, *Acta Cryst D*, 2009, **65**, 148–155.